Assessing distinct patterns of cognitive aging using tissue-specific brain age prediction based on diffusion tensor imaging and brain morphometry

Geneviève Richard [Corresp., 1, 2, 3] , Knut Kolskår [1, 2, 3] , Anne-Marthe Sanders [1, 2, 3] , Tobias Kaufmann [1] , Anders Petersen [4] , Nhat Trung Doan [1] , Jennifer Monereo Sánchez [1] , Dag Alnæs [1] , Kristine M. Ulrichsen [1, 2, 3] , Erlend S. Dørum [1, 2, 3] , Ole A. Andreassen [1] , Jan Egil Nordvik [3] , Lars T. Westlye [Corresp. 1, 2]

[1] NORMENT, KG Jebsen Centre for Psychosis Research, Division of Mental Health and Addiction, Oslo University Hospital & Institute of Clinical Medicine, University of Oslo, Oslo, Norway

[2] Department of Psychology, University of Oslo, Oslo, Norway

[3] Sunnaas Rehabilitation Hospital HT, Nesodden, Norway

[4] Center for Visual Cognition, Department of Psychology, University of Copenhagen, Copenhagen, Denmark

Corresponding Authors: Geneviève Richard, Lars T. Westlye
Email address: genevieve.richard@medisin.uio.no, l.t.westlye@psykologi.uio.no

Multimodal imaging enables sensitive measures of the architecture and integrity of the human brain, but the high-dimensional nature of advanced brain imaging features poses inherent challenges for the analyses and interpretations. Multivariate age prediction reduces the dimensionality to one biologically informative summary measure with potential for assessing deviations from normal lifespan trajectories. A number of studies documented remarkably accurate age prediction, but the differential age trajectories and the cognitive sensitivity of distinct brain tissue classes have yet to be adequately characterized. Exploring differential brain age models driven by tissue-specific classifiers provides a hitherto unexplored opportunity to disentangle independent sources of heterogeneity in brain biology. We trained machine-learning models to estimate brain age using various combinations of FreeSurfer based morphometry and diffusion tensor imaging based indices of white matter microstructure in 612 healthy controls aged 18-87 years. To compare the tissue-specific brain ages and their cognitive sensitivity we applied each of the 11 models in an independent and cognitively well-characterized sample (n=265, 20-88 years). Correlations between true and estimated age and mean absolute error (MAE) in our test sample were highest for the most comprehensive brain morphometry (r=0.83, CI:0.78-0.86, MAE=6.76 years) and white matter microstructure (r=0.79, CI:0.74-0.83, MAE=7.28 years) models, confirming sensitivity and generalizability. The deviance from the chronological age were sensitive to performance on several cognitive tests for various models, including spatial Stroop and symbol coding, indicating poorer performance in individuals with an over-estimated age. Tissue-specific brain age models provide sensitive measures of brain integrity, with implications for the study of a range of brain disorders.

Assessing distinct patterns of cognitive aging using tissue-specific brain age prediction based on diffusion tensor imaging and brain morphometry

Geneviève Richard[a,b,c,*], Knut Kolskår[a,b,c], Anne-Marthe Sanders[a,b,c] , Tobias Kaufmann[a], Anders Petersen[d], Nhat Trung Doan[a], Jennifer Monereo Sánchez[a], Dag Alnæs[a], Kristine M. Ulrichsen[a,b,c], Erlend S. Dørum[a,b,c], Ole A. Andreassen[a], Jan Egil Nordvik[c], Lars T. Westlye[a,b,*]

[a] NORMENT, KG Jebsen Centre for Psychosis Research, Division of Mental Health and Addiction, Oslo University Hospital & Institute of Clinical Medicine, University of Oslo, Norway
[b] Department of Psychology, University of Oslo, Norway
[c] Sunnaas Rehabilitation Hospital HT, Nesodden, Norway
[d] Center for Visual Cognition, Department of Psychology, University of Copenhagen, Copenhagen, Denmark

*Corresponding authors:
Geneviève Richard & Lars T. Westlye
Email: genevieve.richard@medisin.uio.no, l.t.westlye@psykologi.uio.no
Postal address: Oslo University Hospital, P.O.Box 4956 Nydalen, 0424 OSLO, Norway
Telephone: +47 23 02 73 50, Fax: +47 23 02 73 33

1 **Abstract**

2 Multimodal imaging enables sensitive measures of the architecture and integrity of the human

3 brain, but the high-dimensional nature of advanced brain imaging features poses inherent

4 challenges for the analyses and interpretations. Multivariate age prediction reduces the

5 dimensionality to one biologically informative summary measure with potential for assessing

6 deviations from normal lifespan trajectories. A number of studies documented remarkably

7 accurate age prediction, but the differential age trajectories and the cognitive sensitivity of

8 distinct brain tissue classes have yet to be adequately characterized.

9   Exploring differential brain age models driven by tissue-specific classifiers provides a

10 hitherto unexplored opportunity to disentangle independent sources of heterogeneity in brain

11 biology. We trained machine-learning models to estimate brain age using various combinations

12 of FreeSurfer based morphometry and diffusion tensor imaging based indices of white matter

13 microstructure in 612 healthy controls aged 18-87 years. To compare the tissue-specific brain

14 ages and their cognitive sensitivity we applied each of the 11 models in an independent and

15 cognitively well-characterized sample (n=265, 20-88 years). Correlations between true and

16 estimated age and mean absolute error (MAE) in our test sample were highest for the most

17 comprehensive brain morphometry (r=0.83, CI:0.78-0.86, MAE=6.76 years) and white matter

18 microstructure (r=0.79, CI:0.74-0.83, MAE=7.28 years) models, confirming sensitivity and

19 generalizability. The deviance from the chronological age were sensitive to performance on

20 several cognitive tests for various models, including spatial Stroop and symbol coding, indicating

21 poorer performance in individuals with an over-estimated age. Tissue-specific brain age models

22 provide sensitive measures of brain integrity, with implications for the study of a range of brain

23 disorders.

24 **Introduction**

25 Increasing age is a major risk factor for cognitive decline and neurodegeneration, and deviating

26 lifespan trajectories in brain structure and function is a sensitive marker in several common

27 neurological and mental disorders (Cole & Franke 2017). The maturing and aging brain is highly

28 heterogeneous in term of individual trajectories and in term of brain regions and mechanisms

29 involved (Fjell et al. 2013; Westlye et al. 2010b). Understanding the individual determinants and

30 heterogeneity of the developing and aging brain is imperative for identifying persons at risk for

31 various brain disorders, and for developing and applying effective and targeted treatments.

32   Exploring different modalities acquired by magnetic resonance imaging (MRI) provides a

33 powerful tool to investigate age-related differences in both gray- and white- matter tissue classes

34 across brain regions. However, the richness and complexity of the information provided by

35 advanced imaging pipelines challenges its interpretation. Together, the multifactorial age-related

36 variability and the richness of imaging measures have motivated the development of biologically

37 informative summary measures based on brain imaging data. Using machine learning to estimate

38 the biological age of the brain based on neuroimaging data is one such approach (Cole & Franke

39 2017; Cole et al. 2018; Kaufmann et al. 2018). Deviation from the normative trajectory is a

40 highly relevant biomarker for the integrity of the brain in healthy and clinical populations

41 (Marquand et al. 2016; Wolfers et al. in press). Brain age gap is a heritable trait showing

42 regionally specific genetic overlaps with major brain disorders, including schizophrenia and

43 multiple sclerosis (Kaufmann et al. 2018), and accumulating evidence supports increased brain

44 age in several clinical groups, including patients with schizophrenia (Kaufmann et al. 2018;

45 Schnack et al. 2016), Alzheimer's disease (Amoroso et al. 2017; Kaufmann et al. 2018), HIV

46 (Cole et al. 2017b; Kuhn et al. 2018), multiple sclerosis (Kaufmann et al. 2018), and

47   cardiovascular risk factors (Franke et al. 2013; Habes et al. 2016). Indeed, while individuals with

48   brains estimated as younger than their chronological age have been shown to be more physically

49   active (Steffener et al. 2016), augmented brain age has been associated with poor health (Ronan

50   et al. 2016), poor cognitive performance (Liem et al. 2017), early neurodegenerative diseases

51   (Gaser et al. 2013), and increased mortality (Cole et al. 2017a). Less is known about the

52   biological and regional heterogeneity, i.e. to which degree different brain regions, systems or

53   compartments show differential aging patterns and sensitivity to cognitive performance. Brain

54   gray and white matter compartments, which can be assessed and quantified using T1-weighted

55   imaging and diffusion tensor imaging (DTI), respectively, comprise distinct tissue classes with

56   largely differential biological and environmental modifiers and age trajectories (Bennett et al.

57   2010; Cao et al. 2017; Fjell et al. 2013; Salat et al. 2005; Storsve et al. 2014; Westlye et al.

58   2010a; Westlye et al. 2010b). Therefore, allowing for differential brain age models for these

59   distinct classes provides an opportunity to disentangle independent sources of heterogeneity in

60   brain aging.

61   Thus, to identify common and unique aging patterns with potentially differential

62   sensitivity to cognitive function, we aimed to test the complementary value of tissue-specific

63   prediction by comparing brain age estimated using different combinations of FreeSurfer based

64   morphometric measures (regional cortical thickness, surface area and volume) and white matter

65   microstructure (DTI based fractional anisotropy and mean, radial and axial diffusivity) across the

66   brain. Based on previous studies on brain aging, we expected high accuracy and generalizability

67   of the age prediction models (Cole & Franke 2017). Since tissue specific brain age models

68   capture biologically distinct information, we anticipated that the different FreeSurfer based brain

69   morphometry and white matter microstructure models would only partly reflect common

70   variance, and therefore provide complementary information with differential sensitivity to

71   cognitive performance. Given that brain age predictions might be sensitive to the overall

72   integrity of the brain (Liem et al. 2017), we anticipated that adult individuals in the targeted age

73   range who show and over-estimated brain age would also show lower cognitive performance, in

74   particular among the elderly, and that the tissue-specific brain age models would show partly

75   differential cognitive sensitivity.

76   To ensure generalizability, we trained the models in a large publicly available training set

77   (n=612, 18-87 years) and validated their performance using 10-fold cross-validation before

78   applying to an independent and well characterized test set (n=265, 20-88 years). We assessed the

79   cognitive sensitivity using linear and non-linear models with performance on a range of paper-

80   and-pencil and computerized tests comprising different large-scale cognitive domains

81   (processing speed, executive functioning, working memory, attention, and general intellectual

82   abilities) and cognitive scores based on computational models as dependent variables and age,

83   sex and brain age gap (BAG, estimated brain age minus chronological age) as independent

84   variables. For transparency, we report results both at an uncorrected level and corrected using

85   false discovery rate (FDR) and Bonferroni methods to control the error rate.

86

87   **Materials and methods**

88   Figure 1 displays a flowchart of the main analysis pipeline. Table 1 summarizes key

89   demographics. We included data from healthy volunteers from two independent cohorts: (1) the

90   Cambridge Centre for Ageing and Neuroscience (Cam-CAN) sample (http://www.mrc-

91   cbu.cam.ac.uk/datasets/camcan/; (Shafto et al. 2014; Taylor et al. 2017)) and (2) StrokeMRI,

92   which is an ongoing study on the determinants of stroke recovery, brain health and successful

93   aging (Dorum et al. 2016; Dorum et al. 2017). Figure 2 shows the age distribution for each

94   sample. The distribution of age (t = -2.09, p = 0.037) and sex ($\chi^2(1)$ = 10.92, p < 0.001) differed

95   between samples.

96   Volunteers were recruited to Cam-CAN through a large-scale collaborative research

97   project funded by the Biotechnology and Biological Sciences Research Council (BBSRC, grant

98   number BB/H008217/1), the UK Medical Research Council and University of Cambridge. For

99   more information, see www.cam-can.org. Among the 650 datasets made available, 17 were

100   excluded based on missing or poor quality DTI data and 21 due to poor T1-weighted data

101   quality. Data from the remaining 612 individuals (age 18-87, mean = 54.41, SD = 18.26, 314

102   females) were included.

103   Healthy individuals were recruited to StrokeMRI through advertisement in newspapers,

104   social media and word-of-mouth. All participants completed a comprehensive cognitive

105   assessment, multimodal MRI and blood sampling for clinical biochemical analysis, various

106   biomarkers and genotyping. MRI and cognitive assessments were performed on two subsequent

107   days. Exclusion criteria included history of stroke, dementia, or other neurologic and psychiatric

108   diseases, alcohol- and substance abuse, medications significantly affecting the nervous system

109   and counter indications for MRI. In addition, individuals scoring lower than 25 on the Montreal

110   Cognitive Assessment (MoCA; Nasreddine et al. 2005) were assessed for inclusion based on

111   their age, level of education and performance on other cognitive tests. No participants were

112   excluded based on a single low score. A neuroradiologist reviewed all scans and 14 participants

113   with clinically significant abnormalities were excluded. Additional exclusion criteria included

114   missing or incomplete MRI or cognitive data (n=2), or poor quality images (n=20). The

115   remaining 265 participants (age 20-88, mean = 56.95, SD = 14.84, 168 females) were included in

116   further analyses. The study was supported by the Norwegian ExtraFoundation for Health and

117   Rehabilitation (2015/FO5146), the Research Council of Norway (249795, 248238), the South-

118   Eastern Norway Regional Health Authority (2014097, 2015044, 2015073), Sunnaas

119   Rehabilitation Hospital, and the Department of Psychology, University of Oslo, and approved by

120   the Regional Committee for Medical and Health Research Ethics (South-East Norway, REK

121   2014/694), and conducted in accordance with the Helsinki declaration. All subjects signed an

122   informed consent prior to participating and received a compensation for their participation.

123

124   *- Insert Table 1 and Figure 1 and 2 -*

125

126   *Cognitive assessment in StrokeMRI*

127   Cognitive performance was assessed with a set of neuropsychological and computerized tests

128   assumed to be sensitive to cognitive aging, including the MoCA, the vocabulary and matrix

129   subtests of the Wechsler Abbreviated Scale of Intelligence (WASI; Wechsler 1999), the

130   California Verbal Learning Test (CVLT-II; Delis et al. 2000), and the Delis-Kaplan Executive

131   Function System (D-KEFS) color word interference test (Stroop; Delis et al. 2001). We included

132   several computerized tests from the Cognitive Assessment at Bedside for iPAD (CABPad; Willer

133   et al. 2016), including motor speed, verbal fluency (phonological and semantic), working

134   memory, spatial Stroop (executive control of attention), spatial attention span, and symbol digit

135   coding tests. In addition, in order to assess the specificity of cognitive associations using

136   computation modeling, we included three mathematically independent parameters based on the

137   Theory of Visual Attention (TVA; Bundesen 1990; Bundesen & Habekost 2008), including

138   short-term memory storage (K), processing speed (C), perceptual threshold (t_0). These

139   parameters based on computational modeling of response patterns have been shown to be

140   sensitive to age, brain structure and function in healthy individuals (Espeseth et al. 2014;

141   Wiegand et al. 2018) and a range of brain disorders (Habekost 2015; Habekost & Starrfelt 2009).

142   Here, we used a TVA-based modeling of a whole report (Sperling 1960), in which six letters

143   were briefly presented for different exposure durations and the participant's task was to

144   accurately report as many letters as possible. Task error rate was also assessed (i.e. number of

145   incorrect letters out of reported letters).

146

147   *MRI acquisition*

148   Cam-CAN participants were scanned on a 3T Siemens TIM Trio scanner with a 32-channel

149   head-coil at Medical Research Council (UK) Cognition and Brain Sciences Unit (MRC-CBSU)

150   in Cambridge, UK. DTI data was acquired using a twice-refocused spin echo sequence with the

151   following parameters a repetition time (TR) of 9100 ms, echo time (TE) of 104 ms, field of view

152   (FOV) of 192 x 192 mm, voxel size: 2 mm^3, 66 axial slices using 30 directions with b= 1000

153   s/mm^2, 30 directions with b= 2000 s/mm^2, and 3 b=0 images (Shafto et al. 2014). Only the

154   b=[0,1000] were used in the current analysis. High-resolution 3D T1-weighted data was acquired

155   using a magnetization prepared rapid gradient echo (MPRAGE) sequence with the following

156   parameters: TR: 2250 ms, TE: 2.99 ms, inversion time (TI): 900 ms, flip angle: 9°, FOV of 256 x

157   240 x 192mm; voxel size =1 mm^3 isotropic, GRAPPA acceleration factor of 2, scan time 4:32

158   minutes (Shafto et al. 2014).

159   StrokeMRI participants were scanned on a 3T GE 750 Discovery MRI scanner with a 32-

160   channel head coil at Oslo University Hospital. Paddings were used to reduce head motion. DTI

161   data were acquired using an echo planar imaging (EPI) sequence with the following parameters:

162 TR/TE/flip angle: 8150 ms/83.1 ms/90°, FOV: 256 x 256 mm, slice thickness: 2 mm, in-plane

163 resolution: 2 mm, 60 directions (b=1000 s/mm²) and 5 b=0 volumes, scan time: 8:58 min. In

164 addition, 7 b=0 volumes with reversed phase-encoding direction were acquired. High-resolution

165 T1-weighted data was acquired using a 3D IR-prepared FSPGR (BRAVO) with the following

166 parameters: TR: 8.16 ms, TE: 3.18 ms, flip angle: 12°, voxel size: $1 \times 1 \times 1$ mm, FOV: 256 x 256

167 mm, 188 sagittal slices, scan time: 4:43 minutes.

168

169 *DTI processing and analysis*

170 Diffusion MRI data from both samples were processed locally using the Oxford Center for

171 Functional Magnetic Resonance Imaging of the Brain (FMRIB) Software Library (FSL)

172 (http://www.fmrib.ox.ac.uk/fsl). To correct for geometrical distortions, motion and eddy

173 currents, data were preprocessed using topup (https://fsl.fmrib.ox.ac.uk/fsl/fslwiki/topup) and

174 eddy (https://fsl.fmrib.ox.ac.uk/fsl/fslwiki/eddy) respectively (Andersson et al. 2003; Smith et al.

175 2004). Topup uses information from the reversed phase-encoded image, resulting in pairs of

176 images (blip-up, blip-down) with distortions going in opposite directions. From these image pairs

177 the susceptibility-induced off-resonance field was estimated and the two images were combined

178 into a single corrected one (Andersson et al. 2003; Smith et al. 2004). This step was performed

179 on StrokeMRI data only. Eddy detects and replaces slices affected by signal loss due to bulk

180 motion during diffusion encoding, which is performed within an integrated framework along

181 with correction for susceptibility induced distortions, eddy currents and motion (Andersson &

182 Sotiropoulos 2016). Although these processing steps have been shown to strongly increase the

183 temporal signal-to-noise ratio (tSNR) (Doan et al. 2017), we performed additional visual

184 inspection to identify and remove poor quality data, such as data that failed the processing steps

185 due to low quality.

186   Fractional anisotropy (FA), eigenvector, and eigenvalue maps were calculated using dtifit

187 in FSL. Mean diffusivity (MD) was defined as the mean of all three eigenvalues, radial

188 diffusivity (RD) as the mean of the second and third eigenvalue, and axial diffusivity (AD) as the

189 principal eigenvalue.

190   Voxelwise analysis of FA, MD, AD and RD were carried out using Tract-Based Spatial

191 Statistics (TBSS; Smith et al. 2006), part of FSL (Smith et al. 2004). First, all subjects' FA data

192 were aligned to a common space using the nonlinear registration tool FNIRT (Andersson et al.

193 2007a; Andersson et al. 2007b). Next, the mean FA image was created and thinned to create a

194 mean FA skeleton, which represents the centers of all tracts common to all participants. Each

195 subject's aligned FA data was then projected onto this skeleton and the resulting data fed into

196 voxelwise cross-subject statistics. The same warping and skeletonization was repeated for MD,

197 AD and RD. We thresholded and binarized the mean FA skeleton at FA>0.2. For each

198 individual, we calculated the mean skeleton FA, MD, AD and RD, as well as mean values within

199 23 regions of interest (ROIs) based on two probabilistic white matter atlases provided with FSL,

200 i.e. the CBM-DTI-81 white-matter labels atlas and the JHU white-matter tractography atlas (Hua

201 et al. 2008; Mori et al. 2005; Wakana et al. 2007), yielding a total of 96 DTI features per

202 individual.

203

204 *T1 processing*

205 T1-weighted images from both samples were processed using FreeSurfer 5.3

206 (http://surfer.nmr.mgh.harvard.edu; (Dale et al. 1999)) including brain extraction, intensity

207   normalization, automated tissue segmentation, generation of white and pial surfaces (Dale et al.

208   1999). All reconstructions were visually assessed and edited by trained research personnel where

209   appropriate. The reconstructions that failed the corrections were excluded from further analysis,

210   such as data with excessive movement artefacts. Cortical parcellation was performed using the

211   Desikan–Killiany atlas (Desikan et al. 2006; Fischl et al. 2004) and subcortical segmentation was

212   performed based on a probabilistic atlas (Fischl et al. 2002). In addition to global features

213   (intracranial volume, total surface area, whole-cortex mean thickness), mean thickness, total

214   surface area, and volume for each cortical ROI, as well as the volume of subcortical structures

215   were computed yielding a set of 251 FreeSurfer based features.

216

217   *Age prediction*

218   Eleven different models were trained to estimate age based on the feature sets described above

219   (one based on FreeSurfer T1 features, one based on WM DTI features, one including all T1 and

220   DTI features, in addition to eight models based on a smaller subset of features, including models

221   based on FA, MD, AD, RD, sub-cortical volume, volume, area and thickness to further explore

222   the modality specificity of the estimations).

223   Due to systematic differences in brain features between scanners (Madan 2017) as well as

224   non-linear effects of age, we regressed out main effects of scanner using linear models including

225   age, age squared, sex and scanner for each feature, and used the fitted data in further analysis for

226   brain age prediction. In addition, we regressed out the estimated total intracranial volume from

227   the area and volume features. Next, for each model, we created a training data matrix by

228   concatenating all the features for all participants in the training sample (Cam-CAN), which were

229   used as input to estimate age. We used the *xgboost* framework in R

230   (http://xgboost.readthedocs.io/en/latest/R-package/xgboostPresentation.html), an efficient and

231   scalable implementation of gradient boosting machine learning techniques, to build the

232   prediction models. The following parameters were used: learning rate (eta) = 0.1, nround = 5000,

233   gamma = 1, max_depth = 6, subsample=0.5. To estimate the performance of our models, we

234   used a 10-fold cross-validation procedure within the training sample and repeated the cross-

235   validation step 1000 times to provide a robust estimate of model predictive accuracy. Next, we

236   tested the performance of our trained models by predicting age in unseen healthy subjects in the

237   test sample (StrokeMRI).

238   For each feature set, we calculated the correlation between the predicted and the

239   chronological age as a measure of the model performance, in addition to the mean absolute error

240   (MAE, in years). For each individual, we calculated the discrepancy between the estimated and

241   the chronological age, i.e. the BAG, for each model. The MAE was calculated from the BAG for

242   each model. Since we were interested in the effect of BAG independently of age, the effect of

243   age was regressed out for each BAG using linear models.

244

245   *Statistical analysis*

246   Statistical analysis was performed using R (http://www.r-project.org). For cognitive data, we

247   used *outlierTest* from the car package (Fox & Weisberg 2011) to identify the most extreme

248   observations based on a linear model, including age and sex. Twenty-five observations were

249   identified as outliers and treated as missing values based on a Bonferroni corrected $p < 0.05$. To

250   visualize the associations between the cognitive tests and to form cognitive domain scores based

251   on the correlation patterns, we performed hierarchical clustering using the default setting of the

252   heatmap.2 package in gplots (Warnes et al. 2016), which uses hclust (Müllner 2013) to form

253   clusters based on the complete linkage method. Briefly, this is a step-wise clustering process that

254   merges the two nearest clusters until only one single cluster remains, maximizing distance

255   between individuals components between two clusters.

256   For each cognitive measure and summary score based on the clusters formed form the

257   clustering step above, we used linear models to test for the effect of age and sex. Since cognitive

258   performance may show non-linear associations with age, we performed an additional analysis

259   including both age and age^2 in the models. Then, for each test showing a significant association

260   with age, we tested whether adding BAG to the models lead to an improved model fit. More

261   specifically, we tested for differential associations with cognitive function by comparing the

262   parameter estimates for the different BAG models using Fisher z-transformation. To test the

263   assumption that increased BAG is more relevant for cognitive function among the elderly, we

264   tested for age by BAG interactions on cognitive performance. For transparency, we report both

265   uncorrected p-values and p-values adjusted using FDR (Benjamini & Hochberg 1995; Wright

266   1992) and Bonferroni correction using a factor of 495 (11 brain gaps and 45 cognitive features).

267

268   **Results**

269   *Brain age prediction*

270   10-fold cross-validation on the training sample (Cam-CAN) revealed high correlations between

271   chronological and predicted age for the DTI based white matter microstructure (r=0.87) and

272   FreeSurfer based morphometric (r=0.88) models. Likewise, the correlations for FA (r=.76), MD

273   (r=.80), AD (r=.83), RD (r=78), sub-volume (r=.84), volume (r=.80), area (r=.70) and thickness

274   (r=.79) based models also confirmed reasonable model performance.

275   Most models accurately predicted age in the independent test set (StrokeMRI). Figure 3A

276   shows a correlation matrix for the 11 BAGs. Figure 3B shows the correlations between the

277   chronological age and the predicted age in the test sample for each model with their confidence

278   intervals, ranging from (r=.86, CI:.82-.89, MAE= 6.14) for the combined model to r=.58 (CI:.49-

279   .65, MAE=10.24) for the model based on area. Figure 3C is described below. Figure 3 (D to F)

280   show the estimated age from the three models that performed best among the 11 feature sets, i.e.

281   the combined DTI and T1 feature models (r=.86, CI:.82-.89, MAE= 6.14), the 251 FS T1

282   features (r=.83, CI:.78-.86, MAE= 6.76), and the 96 WM DTI features (r=.79, CI:.74-.83,

283   MAE=7.28).

284

285   *- Insert Figure 3 -*

286

287   *Cognitive assessments and associations with BAGs in StrokeMRI*

288   Figure 4 shows a correlation matrix across all normalized cognitive scores with the variables

289   sorted according to the hierarchical clustering used in the main analysis. Several variables were

290   highly correlated, and the clustering solution generally suggested seven broad cognitive domains

291   including (Cluster 1) memory and learning (CVLT, attention span, MoCA), (Cluster 2) visual

292   processing speed (TVA processing speed and perceptual threshold), (Cluster 3) verbal skills

293   (phonological and semantic flow), (Cluster 4) attentional control and speed (spatial Stroop),

294   (Cluster 5) executive control and speed (color-word Stroop), (Cluster 6) reasoning and

295   psychomotor speed (matrix, symbol coding and motor speed, short-term memory storage (TVA-

296   parameter K)), and (Cluster 7) working memory. Table 1 summarizes descriptive statistics and

297   associations with age and sex for each of the 49 cognitive scores, derived features and domain

298   scores. Linear models revealed 45 significant associations with age after correcting for multiple

299   comparisons, with the strongest effect sizes for the symbol coding test, motor speed, spatial

300   Stroop and spatial attention span. Since non-linear models revealed significant associations with

301   age^2 only with the color word Stroop 3 (inhibition) and its derived scores (See supplementary

302   Table S1), the main models presented here are linear in order to keep the model to its simplest

303   form.

304

305   *- Insert Figure 4 -*

306

307   Table 2 shows summary statistics for the associations between cognitive performance and BAG

308   using linear models, including age and sex as covariates. Figure 5 shows a heatmap of the

309   association between cognitive scores and brain age gaps for which the significant associations

310   have been marked with an asterisk. Supplementary Table S1 and Fig. S1 shows the summary

311   statistics and the heatmap of the associations between cognitive performance and BAG using

312   non-linear models. Figure 3C shows the mean and standard error of the 45 p-values ($-\log_{10}(p)$)

313   for the cognitive scores and composite scores for each row (i.e. BAGs), with a higher mean

314   representing a stronger cumulative association across tests.

315   Figure 6 shows a scatter plot of the 2 strongest associations, which were found between

316   the most comprehensive model (all features combined) and spatial Stroop congruent trials and

317   number of responses, respectively, indicating poorer performance with higher BAG. Fisher z-

318   transformation revealed no statistically significant differences in the cognitive associations

319   between linear models using tissue-specific BAG. No significant interactions were found

320   between BAG and age on cognitive performance.

321

322   *- Insert Figure 5, 6 and Table 2 -*

323

324   **Discussion**

325   Brain aging is highly heterogeneous, and expanding our understanding of the biological

326   determinants of human aging is imperative for reducing the burden of age-related cognitive

327   decline and neurodegenerative disorders. An estimate of an individual's deviation from the

328   expected lifespan trajectory in brain structure and function may provide a sensitive measure of

329   individual brain integrity and health, both in presumably healthy individuals and in patients

330   suffering from various brain disorders.

331   The biological heterogeneity of the brain strongly suggests that the concept of a single

332   brain age is too simple, and that tissue-specific brain age models may provide increased

333   sensitivity and specificity in relation to cognitive and mental functions. In line with this view,

334   our main findings demonstrate that different combinations of FreeSurfer based brain

335   morphometry and DTI based white matter microstructural indices can be used to accurately

336   predict the age of individuals, but that the shared variance from the different models suggest that

337   they reflect partly non-overlapping processes of brain aging. Further, the results revealed partly

338   differential sensitivity to cognitive performance; with the strongest cumulative associations

339   across cognitive tests for brain age gaps estimated using RD. Even though our data provide no

340   strong evidence of independent associations with cognitive performance in the current sample of

341   healthy individuals, tissue specific age prediction models might better inform us about the

342   individual determinants and heterogeneity of the aging brain compared to models collapsing

343   several brain compartments by potentially capturing distinct measures of brain aging.

344

345 *Brain age prediction*

346 For the age prediction models, our results demonstrated that the 11 different combinations of

347 FreeSurfer based morphometric measures (regional cortical thickness, surface area and volume)

348 and white matter microstructure features (diffusion tensor imaging (DTI) based fractional

349 anisotropy and mean, radial and axial diffusivity) across the brain age models accurately

350 predicted the age of an individual with a mean absolute error between 6.14 and 10.23 years.

351 Brain morphometry and white matter microstructure models had a MAE of 6.76 and 7.28

352 respectively, which correspond with previous publications (Cole et al. 2016; Han et al. 2014;

353 Valizadeh et al. 2017). In general, combining features and modalities increased the performance,

354 and the highest performing model included a combination of both brain morphometry and white

355 matter microstructure (mean absolute error of 6.14 years). Moreover, the correlations between

356 the different brain age gaps suggested a relatively low level of shared variance (mean correlation

357 = 0.51, SD=0.13). Together these findings support the notion that tissue specific brain age

358 models capture biologically distinct information. This is in line with the characteristic lifespan

359 patterns of global linear decreases in gray matter volume and the nonlinear trajectories of total

360 white matter volume and DTI based metrics of white matter microstructure (Cox et al. 2016;

361 Fjell et al. 2013; Ge et al. 2002; Liu et al. 2017; Raz et al. 2010; Westlye et al. 2010b),

362 highlighting that the different compartments carry unique biological information and that

363 combining different modalities lead to a better estimation of the age of individuals (Cherubini et

364 al. 2016; Liem et al. 2017; Madan & Kensinger 2018).

365

366 *Cognitive associations*

367   We performed a comprehensive cognitive assessment of the test sample, confirming previous

368   evidence of substantial age-related differences in cognitive performance across a range of tests

369   and domains. Hierarchical clustering of the cognitive features indicated a characteristic pattern of

370   covariance, largely reflecting broad cognitive domains, including memory and learning, visual

371   processing speed, verbal skills, attentional and executive control, reasoning and psychomotor

372   speed, and working memory. Ninety percent of the included cognitive features showed age-

373   differences, with the largest effect sizes observed for speed-based measures, such as symbol

374   coding test, which measures mental and visuo-motor speed (Willer et al. 2016). This is in line

375   with the well-established literature on age-related decline in information processing speed in

376   healthy aging (Bennett et al. 2010; Craik & Salthouse 2008; Harada et al. 2013). Importantly, not

377   only tasks measuring reaction time, but also various TVA measures based on computational

378   modeling, such as short-term memory storage (K), processing speed (C), and perceptual

379   threshold (t_0) showed strong associations with age, in line with previous studies (Espeseth et al.

380   2014; Habekost 2015; Habekost et al. 2013; McAvinue et al. 2012; Wiegand et al. 2018).

381   Based on the assumption that brain age captures variance related to the integrity of the

382   brain, we anticipated that adults with an over-estimated age would show lower cognitive

383   performance, and that the tissue-specific brain age models would show partly differential

384   sensitivity. To test these hypotheses, we used linear models to explore the associations between

385   cognitive performance and BAG, with age and sex as covariates, and directly compared the

386   parameter estimates from the different brain age models. We found a significant association

387   between performance on several tests and BAG beyond the age associations, indicating lower

388   performance in individuals with higher BAG. Briefly, one significant association was found for

389   WM DTI, five for combined BAG, two for the sub-volume, one for the RD and one for the MD

390   BAG. The strongest associations were found with the spatial Stroop congruent trials, and number

391   of responses. These findings support that the deviance between the estimated age and the

392   chronological age captures relevant biological information regarding the cognitive performance

393   of an individual. Whereas we found no significantly different associations between brain age

394   models, the association with symbol digit coding test was only seen for WM DTI BAG, while

395   associations with Stroop 3 and 4 were observed only for sub-volume BAG, suggesting some

396   specificity that should be investigated in future studies including larger samples and a broader

397   spectrum of mental health, cognitive and brain phenotypes, both across healthy and clinical

398   samples. We speculate that the contributions of the different modalities in predicting age and the

399   associations with both cognitive performance, but also age-related illnesses vary across the age-

400   span, as it does during maturational age (Brown et al. 2012). Thus, future studies might benefit

401   from investigating modality specific brain-age estimation using specific age range, including

402   children and adolescents.

403

404   *Limitations*

405   The present findings do not come without limitations. First, although reducing the dimensionality

406   of complex brain imaging data to a biologically informative brain age is a powerful method to

407   assess deviations from normal lifespan trajectories in brain health, findings from this data

408   reduction method are limited in specificity. Here, we attempted to both reduce the complexity of

409   the information while keeping some modality specificity measured by different MRI parameters.

410   Finding a balance between specificity and precision represents an interesting challenge for future

411   studies. Moreover, causality and individual level trajectories cannot be established based on

412   cross-sectional data. Therefore, future longitudinal studies are needed to inform us about the

413   relevance of the differential trajectories of the tissue-specific brain age prediction with

414   implications for the study of a range of brain disorders. Next, although the age distribution of the

415   test sample is irrelevant for the individual prediction accuracy, the relative overrepresentation of

416   older individuals in the test sample is a limitation when investigating interactions between BAG

417   and age. Thus, although the lack of brain by BAG interactions on cognitive function did not

418   support our hypothesis that increased BAG is more relevant for cognitive function among the

419   elderly, future studies including individuals across a broader age range and range of function are

420   needed to characterize the lifespan dynamics in the associations between brain and behavior.

421   More specifically, including children and adolescents would be necessary to characterize the

422   transition between development and aging, i.e. the point of inflection from which the sign of the

423   effects are assumed to change, an important phase that requires further investigations. Moreover,

424   although we covered a relatively broad spectrum of structural brain features, the link between

425   imaging based indices of brain structure and brain function is elusive, and brain age models

426   including other brain imaging features, including functional measures, might provide a sensitive

427   supplement to the current models. Lastly, whereas the results showed some numerical

428   differences in the cognitive sensitivity of the different combinations of FreeSurfer based

429   morphometry and white matter microstructure models, these differences were not statistically

430   significant, and the hypothesis that tissue specific models provide increased specificity in terms

431   of cognitive associations remains to be further explored in future studies.

432   In conclusion, we have demonstrated that models based on different combinations of

433   brain morphometry and white matter microstructural indices provide partly differential

434   information about the aging brain, emphasizing the relevance of tissue-specific brain age models

435   in the study of brain and mental function in health and disease.

436   **References**

437   Amoroso N, Diacono D, Fanizzi A, La Rocca M, Monaco A, Lombardi A, Guaragnella

438   C, Bellotti R, Tangaro S, and Alzheimer's Disease Neuroimaging I. 2017. Deep learning reveals

439   Alzheimer's disease onset in MCI subjects: results from an international challenge. *J Neurosci*

440   *Methods*. 10.1016/j.jneumeth.2017.12.011

441   Andersson JLR, Jenkinson M, and Smith S. 2007a. TR07BP1: Non-linear optimisation.

442   FMRIB Analysis Group Technical Reports: FMRIB Analysis Group.

443   Andersson JLR, Jenkinson M, and Smith S. 2007b. TR07JA2: Non-linear registration,

444   aka spatial normalization. FMRIB Analysis Group Technical Reports: FMRIB Analysis Group.

445   Andersson JLR, Skare S, and Ashburner J. 2003. How to correct susceptibility distortions

446   in spin-echo echo-planar images: application to diffusion tensor imaging. *Neuroimage* 20:870-

447   888. 10.1016/S1053-8119(03)00336-7

448   Andersson JLR, and Sotiropoulos SN. 2016. An integrated approach to correction for off-

449   resonance effects and subject movement in diffusion MR imaging. *Neuroimage* 125:1063-1078.

450   10.1016/j.neuroimage.2015.10.019

451   Benjamini Y, and Hochberg Y. 1995. Controlling the False Discovery Rate - a Practical

452   and Powerful Approach to Multiple Testing. *Journal of the Royal Statistical Society Series B-*

453   *Methodological* 57:289-300.

454   Bennett IJ, Madden DJ, Vaidya CJ, Howard DV, and Howard JH, Jr. 2010. Age-related

455   differences in multiple measures of white matter integrity: A diffusion tensor imaging study of

456   healthy aging. *Hum Brain Mapp* 31:378-390. 10.1002/hbm.20872

457   Brown TT, Kuperman JM, Chung Y, Erhart M, McCabe C, Hagler DJ, Jr., Venkatraman

458   VK, Akshoomoff N, Amaral DG, Bloss CS, Casey BJ, Chang L, Ernst TM, Frazier JA, Gruen

JR, Kaufmann WE, Kenet T, Kennedy DN, Murray SS, Sowell ER, Jernigan TL, and Dale AM.
2012. Neuroanatomical assessment of biological maturity. *Curr Biol* 22:1693-1698.
10.1016/j.cub.2012.07.002

Bundesen C. 1990. A theory of visual attention. *Psychol Rev* 97:523-547.

Bundesen C, and Habekost T. 2008. Principles of Visual Attention: Linking Mind and
Brain. *Oxford University Press*. 10.1093/acprof:oso/9780198570707.001.0001

Cao B, Mwangi B, Passos IC, Wu MJ, Keser Z, Zunta-Soares GB, Xu DP, Hasan KM,
and Soares JC. 2017. Lifespan Gyrification Trajectories of Human Brain in Healthy Individuals
and Patients with Major Psychiatric Disorders. *Scientific Reports* 7. ARTN 511
10.1038/s41598-017-00582-1

Cherubini A, Caligiuri ME, Peran P, Sabatini U, Cosentino C, and Amato F. 2016.
Importance of Multimodal MRI in Characterizing Brain Tissue and Its Potential Application for
Individual Age Prediction. *Ieee Journal of Biomedical and Health Informatics* 20.
10.1109/Jbhi.2016.2559938

Cole JH, and Franke K. 2017. Predicting Age Using Neuroimaging: Innovative Brain
Ageing Biomarkers. *Trends Neurosci*. 10.1016/j.tins.2017.10.001

Cole JH, Marioni RE, Harris SE, and Deary IJ. 2018. Brain age and other bodily 'ages':
implications for neuropsychiatry. *Mol Psychiatry*. 10.1038/s41380-018-0098-1

Cole JH, Poudel RPK, Tsagkrasoulis D, Caan MWA, Steves C, Spector TD, and Montana
G. 2016. Predicting brain age with deep learning from raw imaging data results in a reliable and
heritable biomarker. *ARXIV*. 2016arXiv161202572C

Cole JH, Ritchie SJ, Bastin ME, Valdes Hernandez MC, Munoz Maniega S, Royle N,
Corley J, Pattie A, Harris SE, Zhang Q, Wray NR, Redmond P, Marioni RE, Starr JM, Cox SR,

482   Wardlaw JM, Sharp DJ, and Deary IJ. 2017a. Brain age predicts mortality. *Mol Psychiatry*.

483   10.1038/mp.2017.62

484   Cole JH, Underwood J, Caan MWA, De Francesco D, van Zoest RA, Leech R, Wit

485   FWNM, Portegies P, Geurtsen GJ, Schmand BA, van der Loeff MFS, Franceschi C, Sabin CA,

486   Majoie CBLM, Winston A, Reiss P, Sharp DJ, and Collaboration C. 2017b. Increased brain-

487   predicted aging in treated HIV disease. *Neurology* 88:1349-1357.

488   10.1212/Wnl.0000000000003790

489   Cox SR, Ritchie SJ, Tucker-Drob EM, Liewald DC, Hagenaars SP, Davies G, Wardlaw

490   JM, Gale CR, Bastin ME, and Deary IJ. 2016. Ageing and brain white matter structure in 3,513

491   UK Biobank participants. *Nat Commun* 7:13629. 10.1038/ncomms13629

492   Craik FIM, and Salthouse TA. 2008. *The handbook of aging and cognition*. New York:

493   Psychology Press.

494   Dale AM, Fischl B, and Sereno MI. 1999. Cortical surface-based analysis - I.

495   Segmentation and surface reconstruction. *Neuroimage* 9:179-194. DOI 10.1006/nimg.1998.0395

496   Delis DC, Kaplan E, and Kramer JH. 2001. *Delis-Kaplan Executive Function*

497   *System:Technical Manual*. San Antonio, TX: Harcourt Assessment Company.

498   Delis DC, Kramer JH, Kaplan E, and Ober BA. 2000. *California Verbal Learning Test-*

499   *Second Edition (CVLT-II)*. San Antonio, TX: Psychological Corporation.

500   Desikan RS, Segonne F, Fischl B, Quinn BT, Dickerson BC, Blacker D, Buckner RL,

501   Dale AM, Maguire RP, Hyman BT, Albert MS, and Killiany RJ. 2006. An automated labeling

502   system for subdividing the human cerebral cortex on MRI scans into gyral based regions of

503   interest. *Neuroimage* 31:968-980. 10.1016/j.neuroimage.2006.01.021

504   Doan NT, Engvig A, Persson K, Alnaes D, Kaufmann T, Rokicki J, Cordova-Palomera

505   A, Moberget T, Braekhus A, Barca ML, Engedal K, Andreassen OA, Selbaek G, and Westlye

506   LT. 2017. Dissociable diffusion MRI patterns of white matter microstructure and connectivity in

507   Alzheimer's disease spectrum. *Scientific Reports* 7. ARTN 45131

508   10.1038/srep45131

509   Dorum ES, Alnaes D, Kaufmann T, Richard G, Lund MJ, Tonnesen S, Sneve MH,

510   Mathiesen NC, Rustan OG, Gjertsen O, Vatn S, Fure B, Andreassen OA, Nordvik JE, and

511   Westlye LT. 2016. Age-related differences in brain network activation and co-activation during

512   multiple object tracking. *Brain and Behavior* 6. 10.1002/brb3.533

513   Dorum ES, Kaufmann T, Alnaes D, Andreassen OA, Richard G, Kolskar KK, Nordvik

514   JE, and Westlye LT. 2017. Increased sensitivity to age-related differences in brain functional

515   connectivity during continuous multiple object tracking compared to resting-state. *Neuroimage*

516   148:364-372. 10.1016/j.neuroimage.2017.01.048

517   Espeseth T, Vangkilde SA, Petersen A, Dyrholm M, and Westlye LT. 2014. TVA-based

518   assessment of attentional capacities-associations with age and indices of brain white matter

519   microstructure. *Front Psychol* 5:1177. 10.3389/fpsyg.2014.01177

520   Fischl B, Salat DH, Busa E, Albert M, Dieterich M, Haselgrove C, van der Kouwe A,

521   Killiany R, Kennedy D, Klaveness S, Montillo A, Makris N, Rosen B, and Dale AM. 2002.

522   Whole brain segmentation: Automated labeling of neuroanatomical structures in the human

523   brain. *Neuron* 33:341-355. Doi 10.1016/S0896-6273(02)00569-X

524   Fischl B, van der Kouwe A, Destrieux C, Halgren E, Segonne F, Salat DH, Busa E,

525   Seidman LJ, Goldstein J, Kennedy D, Caviness V, Makris N, Rosen B, and Dale AM. 2004.

526   Automatically parcellating the human cerebral cortex. *Cerebral Cortex* 14:11-22.

527   10.1093/cercor/bhg087

528   Fjell AM, Westlye LT, Grydeland H, Amlien I, Espeseth T, Reinvang I, Raz N, Holland

529   D, Dale AM, Walhovd KB, and Alzheimer Disease Neuroimaging I. 2013. Critical ages in the

530   life course of the adult brain: nonlinear subcortical aging. *Neurobiol Aging* 34:2239-2247.

531   10.1016/j.neurobiolaging.2013.04.006

532   Fox J, and Weisberg S. 2011. An {R} Companion to Applied Regression. In: Second,

533   editor. Thousand Oaks, CA: Sage.

534   Franke K, Gaser C, Manor B, and Novak V. 2013. Advanced BrainAGE in older adults

535   with type 2 diabetes mellitus. *Frontiers in Aging Neuroscience* 5. ARTN 90

536   10.3389/fnagi.2013.00090

537   Gaser C, Franke K, Kloppel S, Koutsouleris N, Sauer H, and Initi AsDN. 2013.

538   BrainAGE in Mild Cognitive Impaired Patients: Predicting the Conversion to Alzheimer's

539   Disease. *PLoS One* 8. ARTN e67346

540   10.1371/journal.pone.0067346

541   Ge Y, Grossman RI, Babb JS, Rabin ML, Mannon LJ, and Kolson DL. 2002. Age-related

542   total gray matter and white matter changes in normal adult brain. Part I: volumetric MR imaging

543   analysis. *AJNR Am J Neuroradiol* 23:1327-1333.

544   Habekost T. 2015. Clinical TVA-based studies: a general review. *Front Psychol* 6:290.

545   10.3389/fpsyg.2015.00290

546   Habekost T, and Starrfelt R. 2009. Visual attention capacity: a review of TVA-based

547   patient studies. *Scand J Psychol* 50:23-32. 10.1111/j.1467-9450.2008.00681.x

548   Habekost T, Vogel A, Rostrup E, Bundesen C, Kyllingsbaek S, Garde E, Ryberg C, and

549   Waldemar G. 2013. Visual processing speed in old age. *Scand J Psychol* 54:89-94.

550   10.1111/sjop.12008

551   Habes M, Guray E, Toledo JB, Zhang T, Bryan RN, Janowitz D, Doshi J, von Sarnowski

552   B, Hegenscheid K, Voelzke H, Schminke U, Hoffmann W, Grabe HJ, and Davatzikos C. 2016.

553   Non-Resilient Brain Aging in Association with Cardiovascular Risk and White Matter

554   Hyperintensities: The Ship Study. *Alzheimer's & Dementia* 12:P226-P227.

555   10.1016/j.jalz.2016.06.407

556   Han CE, Peraza LR, Taylor JP, and Kaiser M. 2014. Predicting Age across Human

557   Lifespan Based on Structural Connectivity from Diffusion Tensor Imaging. *2014 Ieee*

558   *Biomedical Circuits and Systems Conference (Biocas)*:137-140.

559   Harada CN, Natelson Love MC, and Triebel KL. 2013. Normal cognitive aging. *Clin*

560   *Geriatr Med* 29:737-752. 10.1016/j.cger.2013.07.002

561   Hua K, Zhang JY, Wakana S, Jiang HY, Li X, Reich DS, Calabresi PA, Pekar JJ, van Zijl

562   PCM, and Mori S. 2008. Tract probability maps in stereotaxic spaces: Analyses of white matter

563   anatomy and tract-specific quantification. *Neuroimage* 39:336-347.

564   10.1016/j.neuroimage.2007.07.053

565   Kaufmann T, van der Meer D, Doan NT, Schwarz E, Lund MJ, Agartz I, Alnæs D, Barch

566   DM, Baur-Streubel R, Bertolino A, Bettella F, Beyer MK, Bøen E, Borgwardt S, Brandt CL,

567   Buitelaar J, Celius EG, Cervenka S, Conzelmann A, Córdova-Palomera A, Dale AM, de

568   Quervain DJF, Di Carlo P, Djurovic S, Dørum ES, Eisenacher S, Elvsashagen T, Espeseth T,

569   Fatouros-Bergman H, Flyckt L, Franke B, Frei O, Haatveit B, Haberg AK, Harbo HF, Hartman

570   CA, Heslenfeld D, Hoekstra PJ, Høgestøl EA, Jernigan T, Jonassen R, Jönsson EG, Kirsch P,

571 Kloszewska I, Kolskar K-K, Landrø NI, Le Hellard S, Lesch K-P, Lovestone S, Lundervold A,

572 Lundervold AJ, Maglanoc LA, Malt UF, Mecocci P, Melle I, Meyer-Lindenberg A, Moberget T,

573 Norbom LB, Nordvik JE, Nyberg L, Oosterlaan J, Papalino M, Papassotiropoulos A, Pauli P,

574 Pergola G, Persson K, Richard G, Rokicki J, Sanders A-M, Selbæk G, Shadrin AA, Smeland

575 OB, Soininen H, Sowa P, Steen VM, Tsolaki M, Ulrichsen KM, Vellas B, Wang L, Westman E,

576 Ziegler GC, Zink M, Andreassen OA, and Westlye LT. 2018. Genetics of brain age suggest an

577 overlap with common brain disorders. *bioRxiv*.

578   Kuhn T, Kaufmann T, Doan NT, Westlye LT, Jones J, Nunez RA, Bookheimer SY,

579 Singer EJ, Hinkin CH, and Thames AD. 2018. An augmented aging process in brain white

580 matter in HIV. *Hum Brain Mapp*. 10.1002/hbm.24019

581   Liem F, Varoquaux G, Kynast J, Beyer F, Masouleh SK, Huntenburg JM, Lampe L,

582 Rahim M, Abraham A, Craddock RC, Riedel-Heller S, Luck T, Loeffler M, Schroeter ML, Witte

583 AV, Villringer A, and Margulies DS. 2017. Predicting brain-age from multimodal imaging data

584 captures cognitive impairment. *Neuroimage* 148:179-188. 10.1016/j.neuroimage.2016.11.005

585   Liu K, Yao S, Chen K, Zhang J, Yao L, Li K, Jin Z, and Guo X. 2017. Structural Brain

586 Network Changes across the Adult Lifespan. *Front Aging Neurosci* 9:275.

587 10.3389/fnagi.2017.00275

588   Madan CR. 2017. Advances in Studying Brain Morphology: The Benefits of Open-

589 Access Data. *Frontiers in Human Neuroscience* 11. ARTN 405

590   10.3389/fnhum.2017.00405

591   Madan CR, and Kensinger EA. 2018. Predicting age from cortical structure across the

592 lifespan. *Eur J Neurosci* 47:399-416. 10.1111/ejn.13835

593   Marquand AF, Rezek I, Buitelaar J, and Beckmann CF. 2016. Understanding

594   Heterogeneity in Clinical Cohorts Using Normative Models: Beyond Case-Control Studies. *Biol*

595   *Psychiatry* 80:552-561. 10.1016/j.biopsych.2015.12.023

596   McAvinue LP, Habekost T, Johnson KA, Kyllingsbaek S, Vangkilde S, Bundesen C, and

597   Robertson IH. 2012. Sustained attention, attentional selectivity, and attentional capacity across

598   the lifespan. *Atten Percept Psychophys* 74:1570-1582. 10.3758/s13414-012-0352-6

599   Mori S, Wakana S, van Zijl PCM, and Nagae-Poetscher LM. 2005. MRI Atlas of Human

600   White Matter. In: Science E, editor. 1st Edition ed: Elsevier Science. p 276.

601   Müllner D. 2013. {fastcluster}: Fast Hierarchical, Agglomerative Clustering Routines for

602   {R} and {Python}. *Journal of Statistical Software* 53:1-18.

603   Nasreddine ZS, Phillips NA, Bedirian V, Charbonneau S, Whitehead V, Collin I,

604   Cummings JL, and Chertkow H. 2005. The montreal cognitive assessment, MoCA: A brief

605   screening tool for mild cognitive impairment. *Journal of the American Geriatrics Society*

606   53:695-699. DOI 10.1111/j.1532-5415.2005.53221.x

607   Raz N, Ghisletta P, Rodrigue KM, Kennedy KM, and Lindenberger U. 2010. Trajectories

608   of brain aging in middle-aged and older adults: regional and individual differences. *Neuroimage*

609   51:501-511. 10.1016/j.neuroimage.2010.03.020

610   Ronan L, Alexander-Bloch AF, Wagstyl K, Farooqi S, Brayne C, Tyler LK, Fletcher PC,

611   and Cam-CAN. 2016. Obesity associated with increased brain age from midlife. *Neurobiology of*

612   *Aging* 47:63-70. 10.1016/j.neurobiolaging.2016.07.010

613   Salat DH, Tuch DS, Greve DN, van der Kouwe AJW, Hevelone ND, Zaleta AK, Rosen

614   BR, Fischl B, Corkin S, Rosas HD, and Dale AM. 2005. Age-related alterations in white matter

615   microstructure measured by diffusion tensor imaging. *Neurobiology of Aging* 26:1215-1227.

616   10.1016/j.neurobiolaging.2004.09.017

617   Schnack HG, van Haren NE, Nieuwenhuis M, Hulshoff Pol HE, Cahn W, and Kahn RS.

618   2016. Accelerated Brain Aging in Schizophrenia: A Longitudinal Pattern Recognition Study. *Am*

619   *J Psychiatry* 173:607-616. 10.1176/appi.ajp.2015.15070922

620   Shafto MA, Tyler LK, Dixon M, Taylor JR, Rowe JB, Cusack R, Calder AJ, Marslen-

621   Wilson WD, Duncan J, Dalgleish T, Henson RN, Brayne C, Matthews FE, and Cam-CAN. 2014.

622   The Cambridge Centre for Ageing and Neuroscience (Cam-CAN) study protocol: a cross-

623   sectional, lifespan, multidisciplinary examination of healthy cognitive ageing. *Bmc Neurology*

624   14. ARTN 204

625   10.1186/s12883-014-0204-1

626   Smith SM, Jenkinson M, Johansen-Berg H, Rueckert D, Nichols TE, Mackay CE,

627   Watkins KE, Ciccarelli O, Cader MZ, Matthews PM, and Behrens TEJ. 2006. Tract-based spatial

628   statistics: Voxelwise analysis of multi-subject diffusion data. *Neuroimage* 31:1487-1505.

629   10.1016/j.neuroimage.2006.02.024

630   Smith SM, Jenkinson M, Woolrich MW, Beckmann CF, Behrens TEJ, Johansen-Berg H,

631   Bannister PR, De Luca M, Drobnjak I, Flitney DE, Niazy RK, Saunders J, Vickers J, Zhang YY,

632   De Stefano N, Brady JM, and Matthews PM. 2004. Advances in functional and structural MR

633   image analysis and implementation as FSL. *Neuroimage* 23:S208-S219.

634   10.1016/j.neuroimage.2004.07.051

635   Sperling G. 1960. The information available in brief visual presentations. *Psychological*

636   *Monographs: General and Applied* 74:1-29. 10.1037/h0093759

637   Steffener J, Habeck C, O'Shea D, Razlighi Q, Bherer L, and Stern Y. 2016. Differences

638   between chronological and brain age are related to education and self-reported physical activity.

639   *Neurobiology of Aging* 40:138-144. 10.1016/j.neurobiolaging.2016.01.014

640   Storsve AB, Fjell AM, Tamnes CK, Westlye LT, Overbye K, Aasland HW, and Walhovd

641   KB. 2014. Differential Longitudinal Changes in Cortical Thickness, Surface Area and Volume

642   across the Adult Life Span: Regions of Accelerating and Decelerating Change. *Journal of*

643   *Neuroscience* 34:8488-8498. 10.1523/Jneurosci.0391-14.2014

644   Taylor JR, Williams N, Cusack R, Auer T, Shafto MA, Dixon M, Tyler LK, Cam C, and

645   Henson RN. 2017. The Cambridge Centre for Ageing and Neuroscience (Cam-CAN) data

646   repository: Structural and functional MRI, MEG, and cognitive data from a cross-sectional adult

647   lifespan sample. *Neuroimage* 144:262-269. 10.1016/j.neuroimage.2015.09.018

648   Valizadeh SA, Hanggi J, Merillat S, and Jancke L. 2017. Age prediction on the basis of

649   brain anatomical measures. *Hum Brain Mapp* 38:997-1008. 10.1002/hbm.23434

650   Wakana S, Caprihan A, Panzenboeck MM, Fallon JH, Perry M, Gollub RL, Hua KG,

651   Zhang JY, Jiang HY, Dubey P, Blitz A, van Zijl P, and Mori S. 2007. Reproducibility of

652   quantitative tractography methods applied to cerebral white matter. *Neuroimage* 36:630-644.

653   10.1016/j.neuroimage.2007.02.049

654   Warnes GR, Bolker B, Bonebakker L, Gentleman R, Liaw WHA, Lumley T, Maechler

655   M, Magnusson A, Moeller S, Schwartz M, and Venables B. 2016. gplots: Various R

656   Programming Tools for Plotting Data.

657   Wechsler D. 1999. *Wechsler Abbreviated Scale of Intelligence (WASI)*: Psychological

658   Corporation.

659   Westlye LT, Walhovd KB, Dale AM, Bjornerud A, Due-Tonnessen P, Engvig A,

660   Grydeland H, Tamnes CK, Ostby Y, and Fjell AM. 2010a. Differentiating maturational and

661   aging-related changes of the cerebral cortex by use of thickness and signal intensity. *Neuroimage*

662   52:172-185. 10.1016/j.neuroimage.2010.03.056

663   Westlye LT, Walhovd KB, Dale AM, Bjornerud A, Due-Tonnessen P, Engvig A,

664   Grydeland H, Tamnes CK, Ostby Y, and Fjell AM. 2010b. Life-Span Changes of the Human

665   Brain White Matter: Diffusion Tensor Imaging (DTI) and Volumetry. *Cerebral Cortex* 20:2055-

666   2068. 10.1093/cercor/bhp280

667   Wiegand I, Lauritzen MJ, Osler M, Mortensen EL, Rostrup E, Rask L, Richard N,

668   Horwitz A, Benedek K, Vangkilde S, and Petersen A. 2018. EEG correlates of visual short-term

669   memory in older age vary with adult lifespan cognitive development. *Neurobiol Aging* 62:210-

670   220. 10.1016/j.neurobiolaging.2017.10.018

671   Willer L, Pedersen PM, Forchhammer HB, and Christensen HK. 2016. Cognitive

672   assessment at bedside for iPad: A preliminary validation of a novel cognitive test for stroke

673   patients. *European Stroke Journal* 1:294-301. 10.1177/2396987316665233

674   Wolfers T, Doan NT, Kaufmann T, Alnæs D, Moberget T, Agartz I, Buitelaar J, Ueland

675   T, Melle I, Beckmann CF, Franke B, Andreassen OA, Westlye LT, and Marquand A. in press.

676   Extensive interindividual differences in schizophrenia and bipolar disorder: mapping biological

677   heterogeneity in reference to normative brain ageing *JAMA Psychiatry*.

678   Wright SP. 1992. Adjusted P-Values for Simultaneous Inference. *Biometrics* 48:1005-

679   1013. Doi 10.2307/2532694

680

681

682   **Figure legends**

683   **Fig. 1** Flowchart of the main analysis pipeline.

684   **Fig. 2** Histogram of the age distribution for each sample.

685   **Fig. 3** Comparison between the 11 BAG models. (A) Heatmap of the correlation between

686   different BAGs. (B) Correlations between the chronological age and the predicted age in the test

687   sample for each model with their confidence intervals. (C) Mean and standard error of the 45 p-

688   values ($-\log_{10}(p)$) for the cognitive scores and composite scores for each row (i.e. BAGs), with a

689   higher mean representing a stronger global association across tests. (D) Correlation between the

690   chronological age of each subjects and the combined age, (E) the brain morphometry age, and

691   (F) the white matter microstructure age.

692   **Fig. 4** Hierarchical clustering of the cognitive features. Each cognitive score was normalized and

693   when required the scores were multiplied by -1 to ensure that positive scores represent good

694   performance. The higher panel shows the dendrogram resulting from the hierarchical clustering

695   of the scores in 7 cognitive domains. Suppl. table S2 provides detailed overview of all

696   abbreviations used.

697   **Fig. 5** Heatmap of the association between cognitive scores and brain age gaps. The color scale

698   depicts the minus log of the p-values ($-\log_{10}(p)$) for each association. The association marked

699   with a small star represents significant associations after FDR correction, and the one marked

700   with a big star shows significant associations after Bonferroni correction. Suppl. table S2

701   provides detailed overview of all abbreviations used.

702

703   **Fig. 6** Scatter plots of the 2 strongest associations between cognitive measures and BAG. (A)

704   Association between Spatial stroop congruent reaction time and BAG. (B) Association between

705   Spatial stroop number of responses and BAG. The color gradient represents the age where lighter

706   color is assigned to older individuals, and darker color to younger individuals. All associations

707   indicate worse performance with higher brain age gap.

708

709

710

711

712

713

714

715

716

717

718

719

720

721

722

723

724

725

726

727

728 **Table legends**

729 **Table 1.** Demographics and cognitive information. * significant associations between cognitive

730 measures with age after FDR correction, ** significant associations between cognitive measures

731 with age after Bonferroni correction. IQR: interquartile range. MoCA: Montreal Cognitive

732 Assessment. WASI: Wechsler Abbreviated Scale of Intelligence. CVLT: California Verbal

733 Learning Test. STROOP: Delis-Kaplan Executive Function System (D-KEFS) color word

734 interference test. CP: Cognitive Assessment at Bedside for iPAD (CabPAD). WM: working

735 memory. TVA: Theory of Visual Attention. ls: longest serie. ss: sum scores. tot: total.

736

737 **Table 2.** Cognitive associations with Brain Age Gap (BAG) – statistics. * FDR significant **

738 Bonferroni significant. MoCA: Montreal Cognitive Assessment. WASI: Wechsler Abbreviated

739 Scale of Intelligence. CVLT: California Verbal Learning Test. STROOP: Delis-Kaplan

740 Executive Function System (D-KEFS) color word interference test. CP: Cognitive Assessment at

741 Bedside for iPAD (CabPAD). WM: working memory. TVA: Theory of Visual Attention. ls:

742 longest serie. ss: sum scores. tot: total.

743

744

745

746

747

748

749

750

Supplementary Materials

Fig. S1. Heatmap of the association between cognitive scores and brain age gaps using non-linear models, including age, age^2 and sex as covariates. The color scale depicts the minus log of the p-values ($-\log_{10}(p)$) for each association. The association marked with a small star represents significant associations after FDR correction, and the one marked with a big star shows significant associations after Bonferroni correction. Suppl. table S2 provides detailed overview of all abbreviations used.

Table S1. Cognitive associations with Brain Age Gap (BAG) using non-linear models, including age, age^2 and sex as covariates – statistics. * FDR significant ** Bonferroni significant. MoCA: Montreal Cognitive Assessment. WASI: Wechsler Abbreviated Scale of Intelligence. CVLT: California Verbal Learning Test. STROOP: Delis-Kaplan Executive Function System (D-KEFS) color word interference test. CP: Cognitive Assessment at Bedside for iPAD (CabPAD). WM: working memory. TVA: Theory of Visual Attention. ls: longest serie. ss: sum scores. tot: total.

Table S2. List of abbreviations used in Figures 4, 5 and S1. WASI= Wechsler Abbreviated Scale of Intelligence, CLVT= California Verbal Learning Test, STROOP= Delis-Kaplan Executive Function System (D-KEFS) color word interference test, CP= Cognitive Assessment at Bedside for iPAD (CabPAD), TVA= Theory of Visual Attention.

Figure 1

Flowchart of the main analysis pipeline.
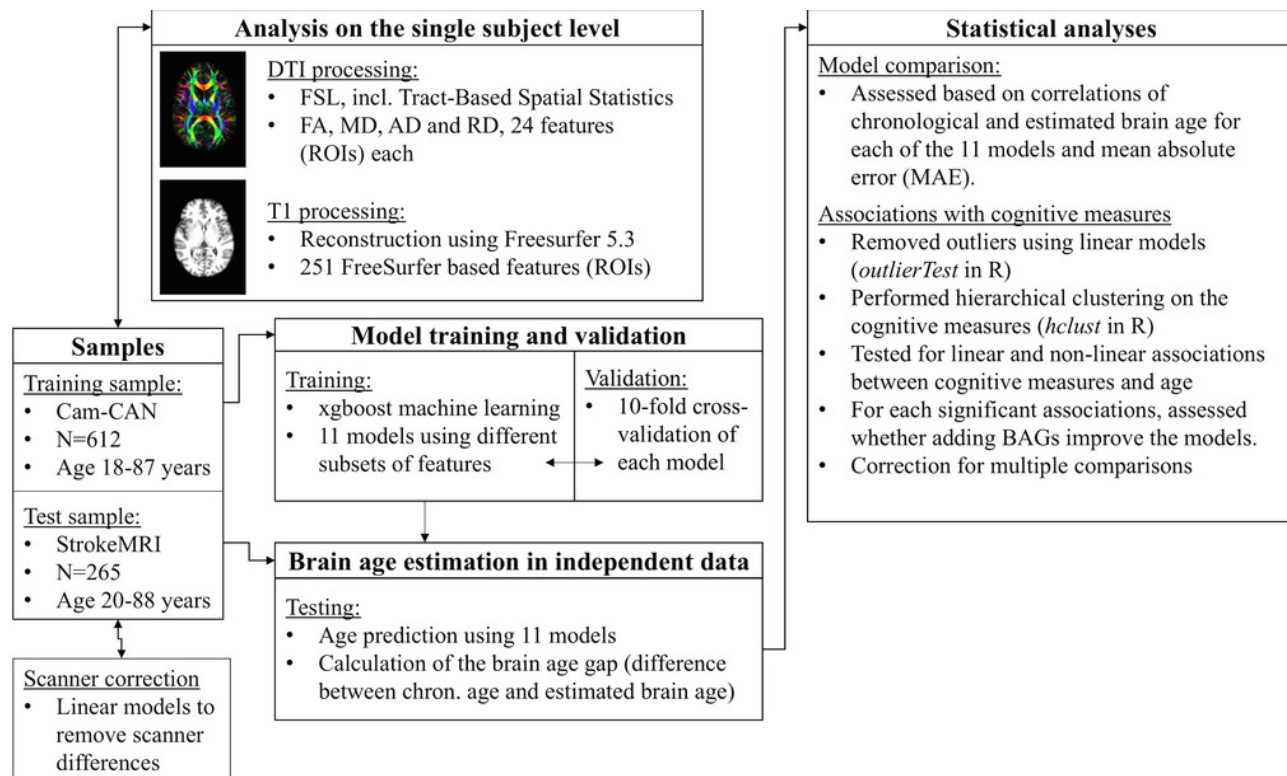
Figure 2

Histogram of the age distribution for each sample.
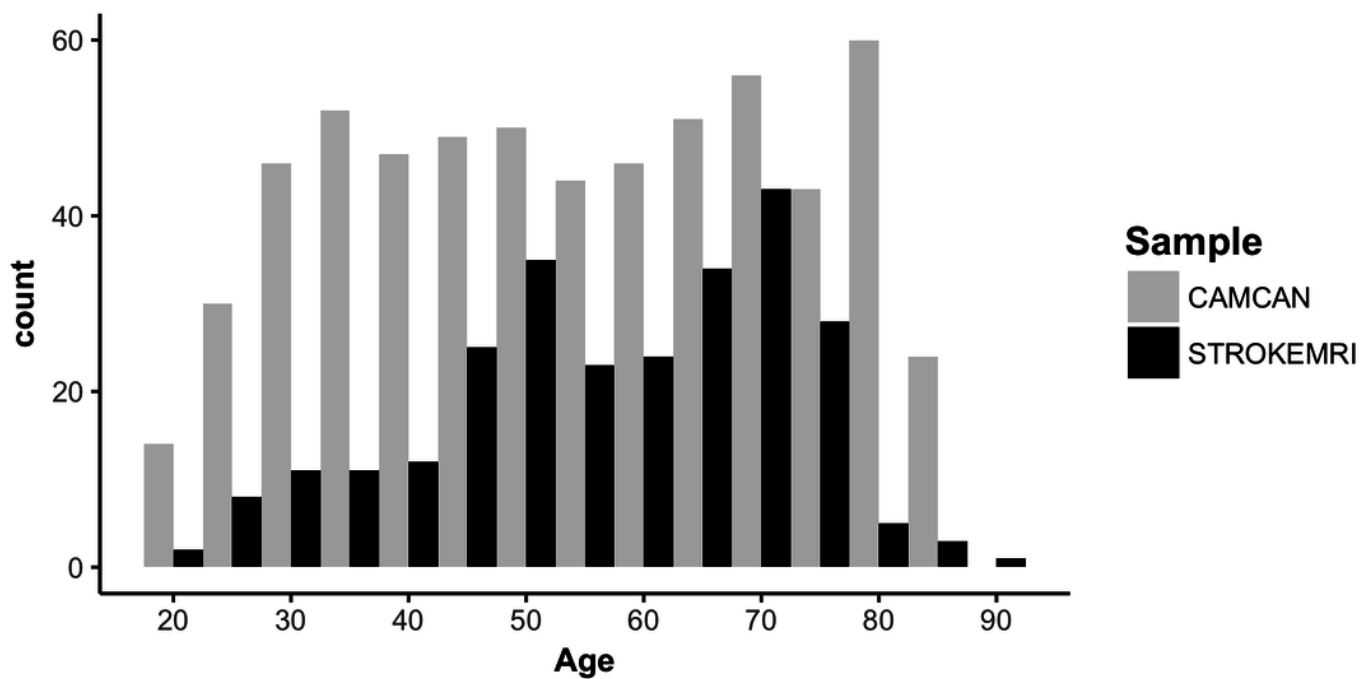
Figure 3

Comparison between the 11 BAG models.

(A) Heatmap of the correlation between different BAGs. (B) Correlations between the chronological age and the predicted age in the test sample for each model with their confidence intervals. (C) Mean and standard error of the 45 p-values ($-\log_{10}(p)$) for the cognitive scores and composite scores for each row (i.e. BAGs), with a higher mean representing a stronger global association across tests. (D) Correlation between the chronological age of each subjects and the combined age, (E) the brain morphometry age, and (F) the white matter microstructure age.
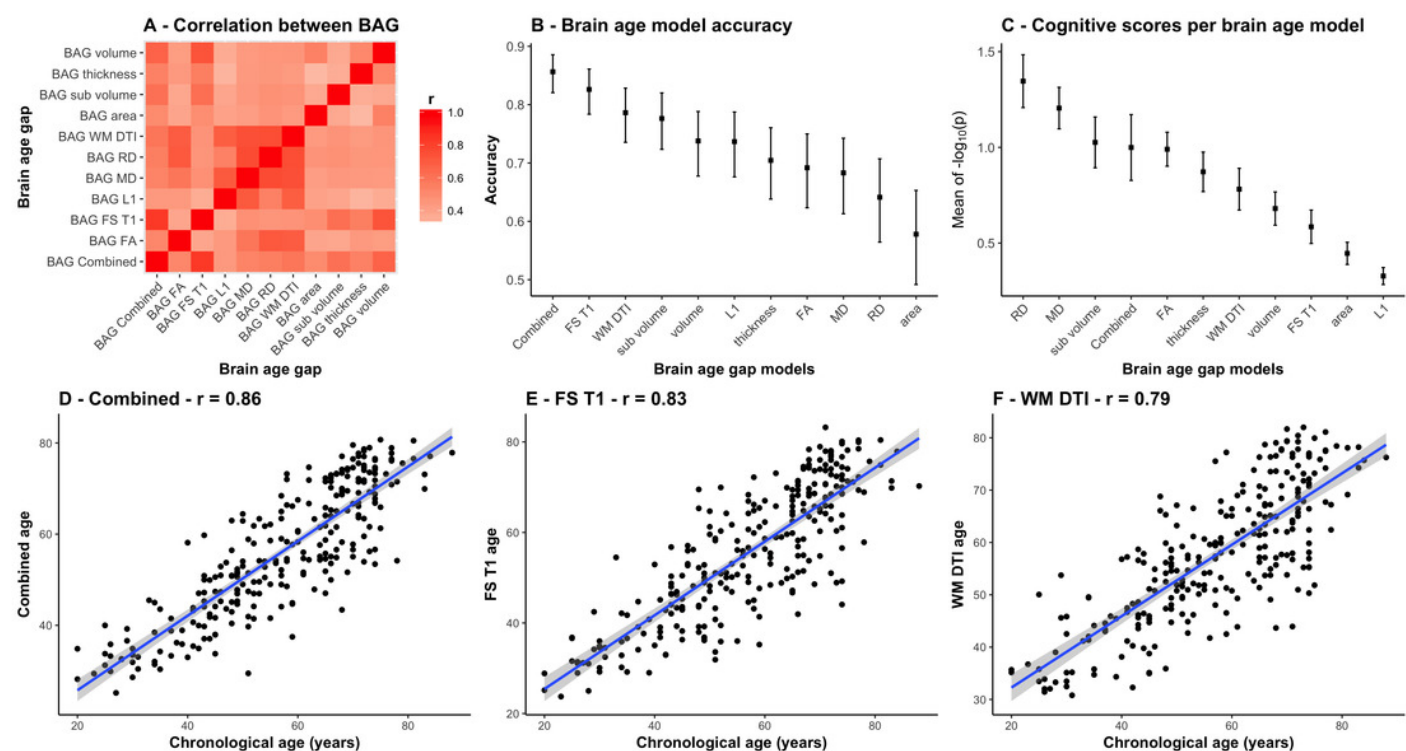
Hierarchical clustering of the cognitive features.

Each cognitive score was normalized and when required the scores were multiplied by -1 to ensure that positive scores represent good performance. The higher panel shows the dendrogram resulting from the hierarchical clustering of the scores in 7 cognitive domains. Suppl. table S2 provides detailed overview of all abbreviations used.
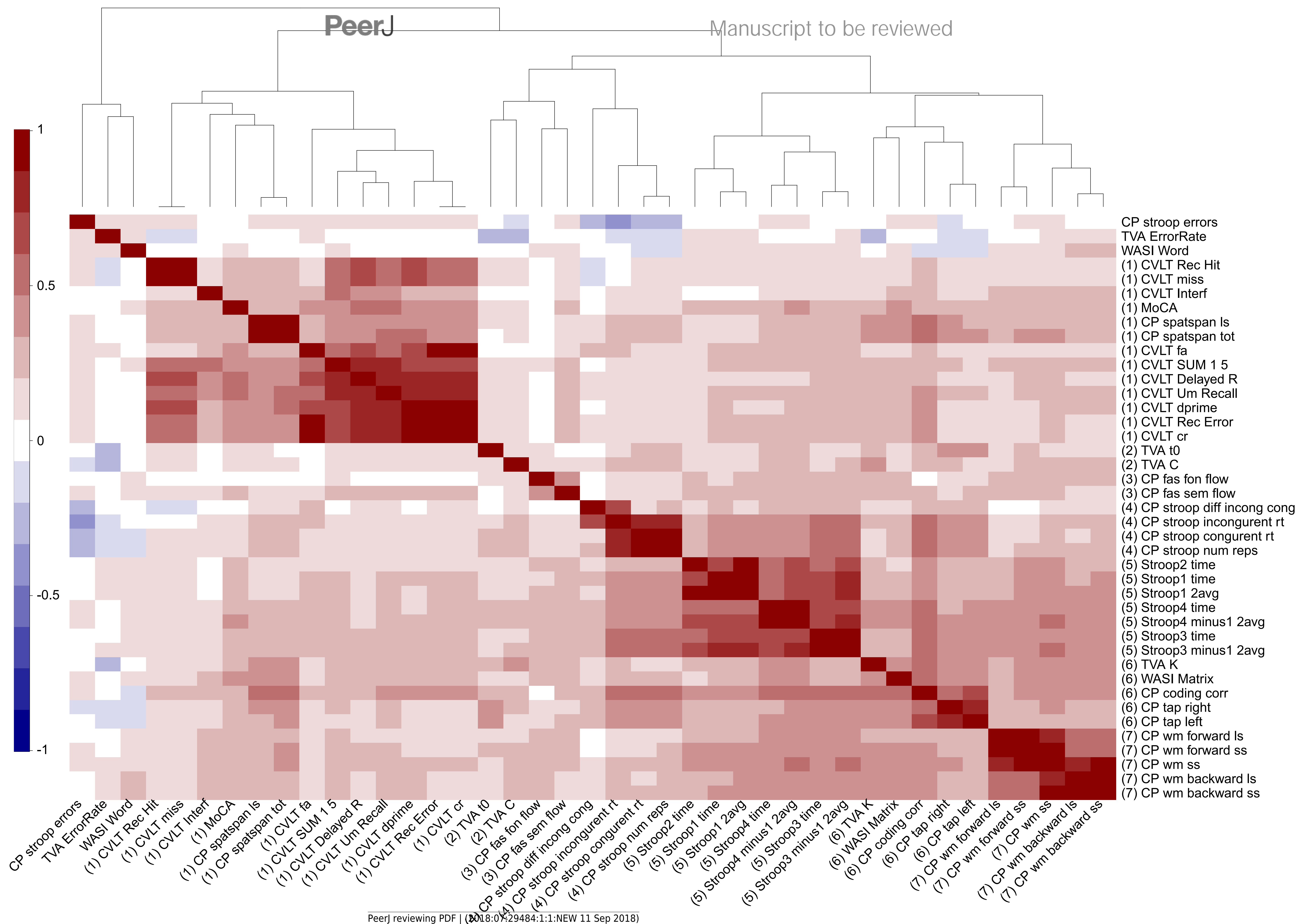
Figure 5

Heatmap of the association between cognitive scores and brain age gaps.

The color scale depicts the minus log of the p-values (-log$_{10}$(p)) for each association. The association marked with a small star represents significant associations after FDR correction, and the one marked with a big star shows significant associations after Bonferroni correction. Suppl. table S2 provides detailed overview of all abbreviations used.
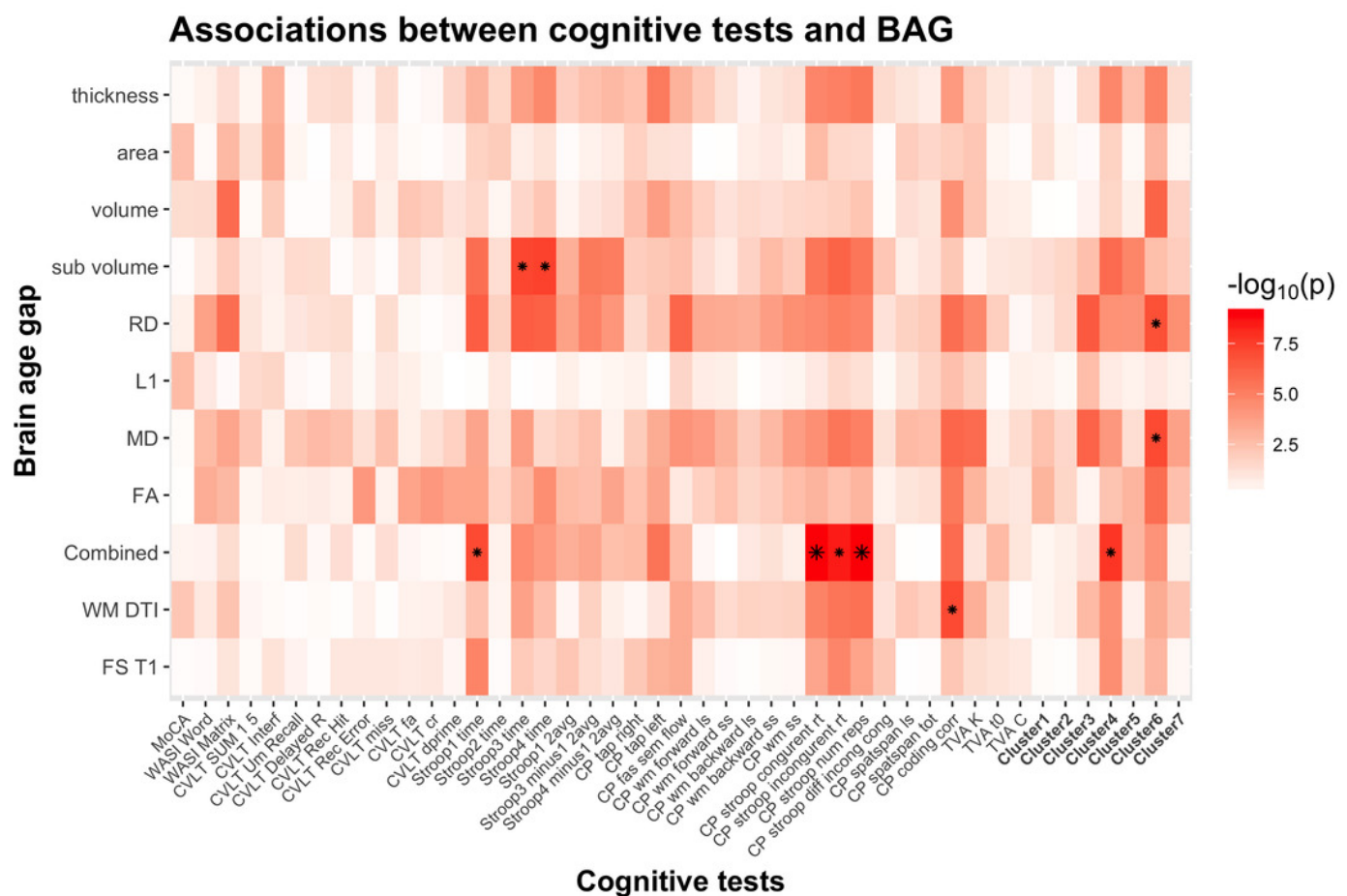
Figure 6

Scatter plots of the 2 strongest associations between cognitive measures and BAG.

(A) Association between Spatial stroop congruent reaction time and BAG. (B) Association between Spatial stroop number of responses and BAG. The color gradient represents the age where lighter color is assigned to older individuals, and darker color to younger individuals. All associations indicate worse performance with higher brain age gap.

Demographics and cognitive information.

* significant associations between cognitive measures with age after FDR correction, ** significant associations between cognitive measures with age after Bonferroni correction. IQR: interquartile range. MoCA: Montreal Cognitive Assessment. WASI: Wechsler Abbreviated Scale of Intelligence. CVLT: California Verbal Learning Test. STROOP: Delis-Kaplan Executive Function System (D-KEFS) color word interference test. CP: Cognitive Assessment at Bedside for iPAD (CabPAD). WM: working memory. TVA: Theory of Visual Attention. ls: longest serie. ss: sum scores. tot: total.

	Cam-CAN	StrokeMRI Mean (SD)	Range (IQR)	Main effect Age t (p)	Main effect Sex t (p)
Total N (% females)	612 (51.3%)	265 (63.4%)			
Mean age (SD)	54.41 (18.26)	56.95 (14.84)			
Age range	18-87	20-88			
MoCA	-	27.60 (1.72)	21 – 30 (2)	-4.57 (<0.001)**	-2.32 (0.021)
WASI words	-	65.27 (6.60)	44 – 79 (10)	4.72 (<0.001)**	0.10 (0.920)
WASI matrix	-	25.39 (5.64)	7 – 35 (6)	-7.60 (<0.001)**	-0.28 (0.776)
CVLT learning 1-5	-	48.92 (11.37)	17 – 73 (15.5)	-5.05 (<0.001)**	-5.26 (<0.001)
CVLT interference	-	5.53 (2.15)	0 – 13 (3)	-4.33 (<0.001)**	-0.41 (0.681)
CVLT recall	-	10.83 (3.42)	0 – 16 (5)	-6.50 (<0.001)**	5.94 (<0.001)
CVLT delayed recall	-	11.39 (3.44)	0 – 16 (5)	-4.97 (<0.001)**	-5.51 (<0.001)
CVLT recognition hit	-	14.70 (1.50)	8 – 16 (2)	-2.62 (0.0093)*	-2.68 (0.008)
CVLT recognition errors	-	3.79 (3.92)	0 – 18 (4)	5.22 (<0.001)**	4.18 (<0.001)
CVLT recog misses	-	1.30 (1.49)	0 – 8 (2)	2.62 (0.0093)*	2.68 (0.008)
CVLT recog false alarm	-	2.46 (3.48)	0 – 18 (3)	4.45 (<0.001)**	3.59 (0.0004)
CVLT recog correct rejection	-	44.20 (3.92)	30 – 48 (4)	-5.22 (<0.001)**	-4.18 (<0.001)
CVLT d'	-	2.97 (0.72)	0.97 – 3.90 (1.11)	-5.01 (<0.001)**	-4.50 (<0.001)
STROOP 1	-	31.14 (5.66)	21 – 50 (7)	5.05 (<0.001)**	2.44 (0.015)
STROOP 2	-	22.12 (3.49)	14 – 35 (4)	2.89 (0.004)*	2.27 (0.024)
STROOP 3	-	55.86 (14.13)	10 – 108 (15)	7.55 (<0.001)**	2.97 (0.003)
STROOP 4	-	61.74 (14.85)	33 – 117 (19)	7.51 (<0.001)**	1.77 (0.078)
STROOP mean 1 and 2	-	26.54 (4.16)	18.5 – 42 (5)	4.47 (<0.001)**	2.47 (0.014)
STROOP 3 minus mean 1 and 2	-	81.94 (16.51)	34.5 – 145 (18.5)	7.31 (<0.001)**	3.02 (0.003)
STROOP 4 minus mean 1 and 2	-	87.64 (16.73)	53.5 – 142 (24)	7.52 (<0.001)**	1.85 (0.066)
CP – Right motor speed	-	79.56 (23.34)	34 – 153 (32)	-12.25 (<0.001)**	-0.36 (0.716)
CP – Left motor speed	-	81.36 (17.80)	39 – 131 (26)	-12.07 (<0.001)**	0.20 (0.842)
CP – FAS Phonological flow	-	54.70 (14.53)	14 – 95 (19.75)	-0.61 (0.541)	-2.58 (0.011)

CP – FAS Semantic flow	-	51.00 (10.14)	27 – 81 (13)	-2.93 (0.004)*	-3.93 (<0.001)
CP – Visual WM forward ls	-	4.23 (1.01)	2 – 7 (2)	-5.31 (<0.001)**	0.29 (0.774)
CP – Visual WM forward ss	-	5.45 (1.87)	1 – 10 (3)	-6.59 (<0.001)**	-0.25 (0.803)
CP – Visual WM backward ls	-	3.80 (1.28)	0 – 8 (1)	-4.60 (<0.001)**	-1.85 (0.065)
CP – Visual WM backward ss	-	4.56 (2.08)	0 – 12 (3)	-5.48 (<0.001)**	-1.02 (0.309)
CP – Visual WM ss	-	9.96 (3.57)	1 – 21 (4)	-7.04 (<0.001)**	-0.95 (0.342)
CP – Spatial stroop congruent (ms)	-	674.42 (132.77)	410 – 1159 (181)	8.52 (<0.001)**	-1.03 (0.304)
CP – Spatial stroop incongruent (ms)	-	929.52 (198.01)	462 – 1827 (269)	9.41 (<0.001)**	-0.75 (0.451)
CP – Spatial stroop Errors	-	2.17 (2.41)	0 – 11 (3)	0.73 (0.463)	1.59 (0.113)
CP – Spatial stroop numb of reps	-	119.63 (16.64)	55 – 166 (22)	-9.67 (<0.001)**	1.23 (0.219)
CP – Spatial stroop incong – cong (ms)	-	252 (110)	20 – 678 (134.5)	5.73 (<0.001)**	-0.68 (0.498)
CP – Spatspan ls	-	5.37 (1.78)	1 – 10 (2)	-9.12 (<0.001)**	-4.88 (<0.001)
CP – Spatspan tot	-	29.87 (12.43)	3 – 55 (18)	-9.28 (<0.001)**	-4.66 (<0.001)
CP – Coding corr	-	54.50 (12.11)	24 – 88 (16)	-16.69 (<0.001)**	-2.46 (0.015)
CP – Coding error	-	0.67 (0.99)	0 – 5 (1)	-1.10 (0.271)	1.56 (0.121)
TVA – Short-term memory storage (K)	-	3.38 (0.77)	1.46 – 5.53 (1.09)	-7.75 (<0.001)**	-1.52 (0.129)
TVA – Processing speed (C)	-	31.55 (14.07)	5.99 – 89.67 (14.75)	-4.69 (<0.001)**	0.41 (0.6847)
TVA – Perceptual threshold (t_0)	-	23.01 (14.05)	0 – 79.75 (17.59)	5.72 (<0.001)**	-1.94 (0.053)
TVA – Error rate	-	0.10 (0.06)	0.0035 – 0.3316 (0.0983)	-1.35 (0.177)	0.67 (0.502)
Cluster 1	-	-	-	-7.19 (<0.001)**	-5.16 (<0.001)
Cluster 2	-	-	-	-7.28 (<0.001)**	1.61 (0.110)
Cluster 3	-	-	-	-2.01 (0.045)*	-3.99 (<0.001)
Cluster 4	-	-	-	-9.98 (<0.001)**	1.25 (0.212)
Cluster 5	-	-	-	-6.86 (<0.001)**	-2.56 (0.011)
Cluster 6	-	-	-	-15.79 (<0.001)**	-1.08 (0.282)
Cluster 7	-	-	-	-6.50 (<0.001)**	-0.77 (0.440)

3   Table 1. Demographics and cognitive information. * significant associations between cognitive

4   measures with age after FDR correction, ** significant associations between cognitive measures

5   with age after Bonferroni correction. IQR: interquartile range. MoCA: Montreal Cognitive

6   Assessment. WASI: Wechsler Abbreviated Scale of Intelligence. CVLT: California Verbal

7   Learning Test. STROOP: Delis-Kaplan Executive Function System (D-KEFS) color word

8   interference test. CP: CabPad. WM: working memory. TVA: Theory of Visual Attention. ls:

9   longest serie. ss: sum scores. tot: total.

Cognitive associations with Brain Age Gap (BAG) – statistics.

* FDR significant ** Bonferroni significant. MoCA: Montreal Cognitive Assessment. WASI: Wechsler Abbreviated Scale of Intelligence. CVLT: California Verbal Learning Test. STROOP: Delis-Kaplan Executive Function System (D-KEFS) color word interference test. CP: Cognitive Assessment at Bedside for iPAD (CabPAD). WM: working memory. TVA: Theory of Visual Attention. ls: longest serie. ss: sum scores. tot: total.

Test	Adj R² no-BAG	BAG	Main effect Age t (p)	Main effect Sex t (p)	Main effect BAG t (p)	Adj R²
MoCA	0.0907	T1	-4.5596 (<0.001)	-2.3145 (0.021)	-0.124 (0.901)	0.0878
		DTI	-4.5599 (<0.001)	-2.3155 (0.021)	1.5914 (0.113)	0.0966
		Combined	-4.5653 (<0.001)	-2.3176 (0.021)	-0.4626 (0.644)	0.0885
WASI words	0.0731	T1	4.7118 (<0.001)	0.1020 (0.919)	-0.2169 (0.828)	0.0704
		DTI	4.7056 (<0.001)	0.1121 (0.911)	-0.8126 (0.417)	0.0727
		Combined	4.7091 (<0.001)	0.1041 (0.917)	-0.4827 (0.630)	0.0711
WASI matrix	0.1791	T1	-7.6061 (<0.001)	-0.2785 (0.781)	-0.9158 (0.361)	0.1793
		DTI	-7.6610 (<0.001)	-0.2624 (0.793)	-1.6546 (0.099)	0.1854
		Combined	-7.6128 (<0.001)	-0.2726 (0.785)	-1.1102 (0.268)	0.1806
CVLT learning 1-5	0.1810	T1	-5.0373 (<0.001)	-5.2514 (<0.001)	-0.2505 (0.802)	0.1750
		DTI	-5.0418 (<0.001)	-5.2533 (<0.001)	-0.3608 (0.719)	0.1753
		Combined	-5.0387 (<0.001)	-5.2522 (<0.001)	-0.2492 (0.803)	0.1750
CVLT interference	0.0664	T1	-4.3256 (<0.001)	-0.4062 (0.685)	-0.9588 (0.339)	0.0626
		DTI	-4.3218 (<0.001)	-0.4104 (0.682)	-0.2391 (0.811)	0.0594
		Combined	-4.3202 (<0.001)	-0.4101 (0.682)	-0.1875 (0.851)	0.0594
CVLT recall	0.2438	T1	-6.4897 (<0.001)	-5.9257 (<0.001)	-0.4868 (0.627)	0.2397
		DTI	-6.4885 (<0.001)	-5.9257 (<0.001)	-0.1245 (0.901)	0.2391
		Combined	-6.5080 (<0.001)	-5.9373 (<0.001)	-1.1114 (0.268)	0.2427
CVLT delayed recall	0.1850	T1	-4.9636 (<0.001)	-5.4973 (<0.001)	0.1421 (0.887)	0.1808
		DTI	-4.9611 (<0.001)	-5.4969 (<0.001)	0.224 (0.823)	0.1809
		Combined	-4.9655 (<0.001)	-5.4954 (<0.001)	-0.3038 (0.762)	0.1810
CVLT recognition hits	0.0494	T1	-2.6125 (0.010)	-2.6822 (0.008)	-0.8586 (0.391)	0.0486
		DTI	-2.6144 (0.010)	-2.6786 (0.008)	0.0946 (0.925)	0.0459
		Combined	-2.6212 (0.009)	-2.6854 (0.008)	-1.0724 (0.285)	0.0501
CVLT recognition errors	0.1526	T1	5.2227 (<0.001)	4.1850 (<0.001)	-0.8471 (0.398)	0.1528
		DTI	5.2115 (<0.001)	4.1755 (<0.001)	-0.5651 (0.573)	0.1514
		Combined	5.2139 (<0.001)	4.1740 (<0.001)	-0.2537 (0.800)	0.1506
CVLT recog misses	0.0494	T1	2.6125 (0.010)	2.6822 (0.008)	0.8586 (0.391)	0.0486
		DTI	2.6144 (0.010)	2.6786 (0.008)	-0.0946 (0.925)	0.0459
		Combined	2.6212 (0.009)	2.6854 (0.008)	1.0724 (0.285)	0.0501
CVLT recog false alarm	0.1150	T1	4.4519 (<0.001)	3.5827 (<0.001)	-0.776 (0.439)	0.1146
		DTI	4.4378 (<0.001)	3.5803 (<0.001)	-0.5207 (0.603)	0.1134
		Combined	4.4418 (<0.001)	3.5788 (<0.001)	-0.3488 (0.728)	0.1129
CVLT recog correct rejection	0.1526	T1	-5.2227 (<0.001)	-4.1850 (<0.001)	0.8471 (0.398)	0.1528
		DTI	-5.2115 (<0.001)	-4.1755 (<0.001)	0.5651 (0.573)	0.1514
		Combined	-5.2139 (<0.001)	-4.1740 (<0.001)	0.2537 (0.800)	0.1506
CVLT d'	0.1566	T1	-5.0074 (<0.001)	-4.4914 (<0.001)	0.3628 (0.717)	0.1536
		DTI	-5.0021 (<0.001)	-4.4969 (<0.001)	0.8538 (0.394)	0.1556

		Combined	-5.0038 (<0.001)	-4.4902 (<0.001)	0.1699 (0.865)	0.1533
STROOP 1	0.1118	T1	5.1466 (<0.001)	2.4999 (0.013)	2.6939 (0.008)	0.1299
		DTI	5.0968 (<0.001)	2.4769 (0.014)	1.6664 (0.097)	0.1147
		Combined	5.2111 (<0.001)	2.5317 (0.012)	3.3767 (<0.001)*	0.1434
STROOP 2	0.0477	T1	2.8868 (0.004)	2.2619 (0.025)	0.1557 (0.876)	0.0433
		DTI	2.8768 (0.004)	2.2489 (0.025)	-0.4639 (0.643)	0.0440
		Combined	2.8949 (0.004)	2.2713 (0.024)	0.4976 (0.619)	0.0442
STROOP 3	0.2104	T1	7.5930 (<0.001)	2.9898 (0.003)	1.5092 (0.133)	0.2109
		DTI	7.6511 (<0.001)	3.0224 (0.003)	2.231 (0.027)	0.2190
		Combined	7.6793 (<0.001)	3.0233 (0.003)	2.5768 (0.011)	0.2240
STROOP 4	0.1887	T1	7.5403 (<0.001)	1.7884 (0.075)	1.2397 (0.216)	0.1906
		DTI	7.5847 (<0.001)	1.8121 (0.071)	1.7368 (0.084)	0.1953
		Combined	7.6387 (<0.001)	1.8247 (0.069)	2.3662 (0.019)	0.2033
STROOP mean 1 and 2	0.0949	T1	4.5089 (<0.001)	2.5033 (0.013)	1.5875 (0.114)	0.0978
		DTI	4.4750 (<0.001)	2.4760 (0.014)	0.3927 (0.695)	0.0894
		Combined	4.5432 (<0.001)	2.5399 (0.012)	2.0254 (0.044)	0.1034
STROOP 3 minus mean 1 and 2	0.2051	T1	7.3383 (<0.001)	3.0427 (0.003)	1.1397 (0.256)	0.2021
		DTI	7.3613 (<0.001)	3.0703 (0.002)	1.3546 (0.177)	0.2038
		Combined	7.4197 (<0.001)	3.1063 (0.002)	2.1881 (0.030)	0.2130
STROOP 4 minus mean 1 and 2	0.1936	T1	7.5360 (<0.001)	1.8671 (0.063)	0.8763 (0.382)	0.1919
		DTI	7.5297 (<0.001)	1.8697 (0.063)	0.6331 (0.527)	0.1907
		Combined	7.6081 (<0.001)	1.9215 (0.056)	1.7531 (0.081)	0.1993
CP – Right motor speed	0.3695	T1	-12.2893 (<0.001)	-0.3592 (0.720)	-1.5504 (0.122)	0.3676
		DTI	-12.2318 (<0.001)	-0.3612 (0.718)	-0.3435 (0.732)	0.3620
		Combined	-12.3125 (<0.001)	-0.3587 (0.720)	-1.8139 (0.071)	0.3697
CP – Left motor speed	0.3630	T1	-12.1437 (<0.001)	0.2100 (0.834)	-1.9945 (0.047)	0.3634
		DTI	-12.0669 (<0.001)	0.2081 (0.835)	-0.8704 (0.385)	0.3555
		Combined	-12.2516 (<0.001)	0.2149 (0.830)	-2.9047 (0.004)	0.3740
CP – FAS Semantic flow	0.0840	T1	-2.9562 (0.003)	-3.9454 (<0.001)	-2.0826 (0.038)	0.0960
		DTI	-2.9607 (0.003)	-3.9388 (<0.001)	-2.0997 (0.037)	0.0963
		Combined	-2.9513 (0.004)	-3.9389 (<0.001)	-1.8308 (0.068)	0.0926
CP – Visual WM forward ls	0.0936	T1	-5.3071 (<0.001)	0.2850 (0.776)	-0.5838 (0.560)	0.0906
		DTI	-5.3392 (<0.001)	0.2963 (0.767)	-1.7204 (0.087)	0.0999
		Combined	-5.3059 (<0.001)	0.2853 (0.776)	-0.3127 (0.755)	0.0897
CP – Visual WM forward ss	0.1416	T1	-6.5795 (<0.001)	-0.2502 (0.803)	-0.2158 (0.829)	0.1375
		DTI	-6.6000 (<0.001)	-0.2448 (0.807)	-1.1695 (0.243)	0.1420
		Combined	-6.5786 (<0.001)	-0.2496 (0.803)	-0.02 (0.984)	0.1373
CP – Visual WM backward ls	0.0852	T1	-4.5941 (<0.001)	-1.8511 (0.065)	-0.1047 (0.917)	0.0820
		DTI	-4.6170 (<0.001)	-1.8545 (0.065)	-1.3334 (0.184)	0.0884
		Combined	-4.6051 (<0.001)	-1.8550 (0.065)	-0.8013 (0.424)	0.0843
CP – Visual WM backward ss	0.1022	T1	-5.4741 (<0.001)	-1.0181 (0.310)	-0.2721 (0.786)	0.1015

		DTI	-5.4971 (<0.001)	-1.0179 (0.310)	-1.3043 (0.193)	0.1072
		Combined	-5.4898 (<0.001)	-1.0215 (0.308)	-1.0074 (0.315)	0.1048
CP – Visual WM ss	0.1607	T1	-7.0322 (<0.001)	-0.9515 (0.342)	-0.3013 (0.763)	0.1591
		DTI	-7.0622 (<0.001)	-0.9511 (0.342)	-1.3634 (0.174)	0.1649
		Combined	-7.0399 (<0.001)	-0.9528 (0.342)	-0.6665 (0.506)	0.1603
CP – Spatial stroop congruent	0.2288	T1	8.6156 (<0.001)	-1.0080 (0.314)	2.1921 (0.029)	0.2288
		DTI	8.6687 (<0.001)	-1.0021 (0.317)	2.6995 (0.007)	0.2362
		Combined	8.8278 (<0.001)	-0.9828 (0.327)	3.9007 (<0.001)**	0.2588
CP – Spatial stroop incongruent	0.2548	T1	9.5489 (<0.001)	-0.7429 (0.458)	2.6569 (0.008)	0.2700
		DTI	9.5931 (<0.001)	-0.7587 (0.449)	2.8817 (0.004)	0.2735
		Combined	9.7197 (<0.001)	-0.7378 (0.461)	3.8071 (<0.001)**	0.2903
CP – Spatial stroop numb of reps	0.2731	T1	-9.7755 (<0.001)	1.2211 (0.223)	-2.2212 (0.027)	0.2753
		DTI	-9.8507 (<0.001)	1.2328 (0.219)	-2.9614 (0.003)	0.2859
		Combined	-9.9891 (<0.001)	1.2198 (0.224)	-3.8816 (<0.001)**	0.3027
CP – Spatial stroop incong – cong	0.1012	T1	5.7663 (<0.001)	-0.6595 (0.510)	1.5611 (0.120)	0.1134
		DTI	5.7466 (<0.001)	-0.6678 (0.505)	0.9705 (0.333)	0.1081
		Combined	5.7568 (<0.001)	-0.6584 (0.511)	1.2056 (0.229)	0.1099
CP – Spatspan ls	0.3055	T1	-9.1038 (<0.001)	-4.8656 (<0.001)	-0.032 (0.975)	0.3009
		DTI	-9.1746 (<0.001)	-4.9104 (<0.001)	-1.5749 (0.117)	0.3077
		Combined	-9.1043 (<0.001)	-4.8663 (<0.001)	-0.075 (0.940)	0.3009
CP – Spatspan total	0.3057	T1	-9.2664 (<0.001)	-4.6439 (<0.001)	0.1074 (0.915)	0.3024
		DTI	-9.3260 (<0.001)	-4.6815 (<0.001)	-1.3773 (0.170)	0.3076
		Combined	-9.2686 (<0.001)	-4.6461 (<0.001)	-0.0612 (0.951)	0.3024
CP – Coding corr	0.5387	T1	-16.7647 (<0.001)	-2.5004 (0.013)	-1.6149 (0.108)	0.5352
		DTI	-17.0893 (<0.001)	-2.5467 (0.012)	-3.3998 (<0.001)*	0.5510
		Combined	-17.0071 (<0.001)	-2.5604 (0.011)	-3.0056 (0.003)	0.5467
TVA - Short-term memory storage (K)	0.2013	T1	-7.7691 (<0.001)	-1.5196 (0.130)	-1.1179 (0.265)	0.1981
		DTI	-7.8117 (<0.001)	-1.5383 (0.125)	-2.0302 (0.043)	0.2070
		Combined	-7.7525 (<0.001)	-1.5195 (0.130)	-0.9537 (0.341)	0.1970
TVA - Perceptual threshold (t_0)	0.0764	T1	5.7303 (<0.001)	-1.9470 (0.053)	0.9617 (0.337)	0.1141
		DTI	5.7333 (<0.001)	-1.9444 (0.053)	1.1066 (0.270)	0.1152
		Combined	5.7523 (<0.001)	-1.9587 (0.051)	1.8346 (0.068)	0.1226
TVA - Processing speed (C)	0.1304	T1	-4.6692 (<0.001)	0.3969 (0.692)	0.8093 (0.419)	0.0723
		DTI	-4.6800 (<0.001)	0.4053 (0.686)	0.1402 (0.889)	0.0699
		Combined	-4.6827 (<0.001)	0.3944 (0.694)	0.8916 (0.374)	0.0728
Cluster 1	0.2470	T1	-7.1741 (<0.001)	-5.1567 (<0.001)	-0.1927 (0.847)	0.2440
		DTI	-7.1623 (<0.001)	-5.1410 (<0.001)	0.3683 (0.713)	0.2443
		Combined	-7.1805 (<0.001)	-5.1641 (<0.001)	-0.3879 (0.699)	0.2443
Cluster 2	0.1720	T1	-7.2680 (<0.001)	1.6030 (0.110)	-0.1013 (0.919)	0.1687

		DTI	-7.2785 (<0.001)	1.6062 (0.110)	-0.6549 (0.513)	0.1701
		Combined	-7.2740 (<0.001)	1.6104 (0.109)	-0.6382 (0.524)	0.1700
Cluster 3	0.0698	T1	-2.0177 (0.045)	-3.9824 (<0.001)	-0.8103 (0.419)	0.0686
		DTI	-2.0337 (0.043)	-3.9969 (<0.001)	-1.84 (0.067)	0.0783
		Combined	-2.0185 (0.045)	-3.9877 (<0.001)	-0.9765 (0.330)	0.0697
Cluster 4	0.2783	T1	-10.1319 (<0.001)	1.2314 (0.219)	-2.5436 (0.012)	0.2937
		DTI	-10.1479 (<0.001)	1.2377 (0.217)	-2.5207 (0.012)	0.2933
		Combined	-10.3013 (<0.001)	1.2196 (0.224)	-3.6163 (<0.001)*	0.3113
Cluster 5	0.1772	T1	-6.8872 (<0.001)	-2.5902 (0.010)	-1.1084 (0.269)	0.1779
		DTI	-6.8667 (<0.001)	-2.5805 (0.010)	-0.5825 (0.561)	0.1750
		Combined	-6.9577 (<0.001)	-2.6481 (0.009)	-1.9103 (0.057)	0.1858
Cluster 6	0.5092	T1	-15.9345 (<0.001)	-1.1148 (0.266)	-1.8971 (0.059)	0.5145
		DTI	-15.9719 (<0.001)	-1.1080 (0.269)	-2.0875 (0.038)	0.5160
		Combined	-16.0156 (<0.001)	-1.1196 (0.264)	-2.459 (0.015)	0.5193
Cluster 7	0.1399	T1	-6.4852 (<0.001)	-0.7736 (0.440)	-0.3433 (0.732)	0.1369
		DTI	-6.5210 (<0.001)	-0.7689 (0.443)	-1.6007 (0.111)	0.1452
		Combined	-6.4926 (<0.001)	-0.7759 (0.439)	-0.63 (0.529)	0.1379

2 Table 2. Cognitive associations with BAG – statistics. * FDR significant ** Bonferroni

3 significant. MoCA: Montreal Cognitive Assessment. WASI: Wechsler Abbreviated Scale of

4 Intelligence. CVLT: California Verbal Learning Test. STROOP: Delis-Kaplan Executive

5 Function System (D-KEFS) color word interference test. CP: Cognitive Assessment at Bedside

6 for iPAD (CabPAD). WM: working memory. TVA: Theory of Visual Attention. ls: longest serie.

7 ss: sum scores. tot: total.